

University of Groningen

Genetic variance is associated with susceptibility for cigarette smoke-induced DAMP release in mice

Pouwels, Simon D; Faiz, Alen; den Boef, Lisette E.; Gras, Reneé; van den Berge, Maarten; Boezen, H Marike; Korstanje, Ron; Ten Hacken, Nick H T; van Oosterhout, Antoon J. M.; Heijink, Irene H

Published in:

American Journal of Physiology - Lung Cellular and Molecular Physiology

DOI:

[10.1152/ajplung.00466.2016](https://doi.org/10.1152/ajplung.00466.2016)

IMPORTANT NOTE: You are advised to consult the publisher's version (publisher's PDF) if you wish to cite from it. Please check the document version below.

Document Version

Publisher's PDF, also known as Version of record

Publication date:
2017

[Link to publication in University of Groningen/UMCG research database](#)

Citation for published version (APA):

Pouwels, S. D., Faiz, A., den Boef, L. E., Gras, R., van den Berge, M., Boezen, H. M., Korstanje, R., Ten Hacken, N. H. T., van Oosterhout, A. J. M., Heijink, I. H., & Nawijn, M. C. (2017). Genetic variance is associated with susceptibility for cigarette smoke-induced DAMP release in mice. *American Journal of Physiology - Lung Cellular and Molecular Physiology*, 313(3), L559-L580. <https://doi.org/10.1152/ajplung.00466.2016>

Copyright

Other than for strictly personal use, it is not permitted to download or to forward/distribute the text or part of it without the consent of the author(s) and/or copyright holder(s), unless the work is under an open content license (like Creative Commons).


The publication may also be distributed here under the terms of Article 25fa of the Dutch Copyright Act, indicated by the "Taverne" license. More information can be found on the University of Groningen website: <https://www.rug.nl/library/open-access/self-archiving-pure/taverne-amendment>.

Take-down policy

If you believe that this document breaches copyright please contact us providing details, and we will remove access to the work immediately and investigate your claim.

RESEARCH ARTICLE

Genetic variance is associated with susceptibility for cigarette smoke-induced DAMP release in mice

 Simon D. Pouwels,^{1,2} Alen Faiz,^{1,2} Lisette E. den Boef,¹ René Gras,¹ Maarten van den Berge,^{2,5} H. Marike Boezen,^{2,3} Ron Korstanje,⁴ Nick H. T. ten Hacken,^{2,5} Antoon J. M. van Oosterhout,^{1,2} Irene H. Heijink,^{1,2,5} and Martijn C. Nawijn^{1,2}

¹Department of Pathology and Medical Biology, University Medical Center Groningen, University of Groningen, Groningen, The Netherlands; ²GRIAC Research Institute, University Medical Center Groningen, University of Groningen, Groningen, The Netherlands; ³Department of Epidemiology, University Medical Center Groningen, University of Groningen, Groningen, The Netherlands; ⁴The Jackson Laboratory, Bar Harbor, Maine; and ⁵Department of Pulmonology, University Medical Center Groningen, University of Groningen, Groningen, The Netherlands

Submitted 14 October 2016; accepted in final form 31 May 2017

Pouwels SD, Faiz A, den Boef LE, Gras R, van den Berge M, Boezen HM, Korstanje R, ten Hacken NH, van Oosterhout AJ, Heijink IH, Nawijn MC. Genetic variance is associated with susceptibility for cigarette smoke-induced DAMP release in mice. *Am J Physiol Lung Cell Mol Physiol* 313: L559–L580, 2017. First published June 8, 2017; doi:10.1152/ajplung.00466.2016.—Chronic obstructive pulmonary disease (COPD) is characterized by unresolved neutrophilic airway inflammation and is caused by chronic exposure to toxic gases, such as cigarette smoke (CS), in genetically susceptible individuals. Recent data indicate a role for damage-associated molecular patterns (DAMPs) in COPD. Here, we investigated the genetics of CS-induced DAMP release in 28 inbred mouse strains. Subsequently, in lung tissue from a subset of strains, the expression of the identified candidate genes was analyzed. We tested whether small interfering RNA-dependent knockdown of candidate genes altered the susceptibility of the human A549 cell line to CS-induced cell death and DAMP release. Furthermore, we tested whether these genes were differentially regulated by CS exposure in bronchial brushings obtained from individuals with a family history indicative of either the presence or absence of susceptibility for COPD. We observed that, of the four DAMPs tested, double-stranded DNA (dsDNA) showed the highest correlation with neutrophilic airway inflammation. Genetic analyses identified 11 candidate genes governing either CS-induced or basal dsDNA release in mice. Two candidate genes (*Elac2* and *Ppt1*) showed differential expression in lung tissue on CS exposure between susceptible and nonsusceptible mouse strains. Knockdown of *ELAC2* and *PPT1* in A549 cells altered susceptibility to CS extract-induced cell death and DAMP release. In bronchial brushings, CS-induced expression of *ENOX1* and *ARGHGF11* was significantly different between individuals susceptible or nonsusceptible for COPD. Our study shows that genetic variance in a mouse model is associated with CS-induced DAMP release, and that this might contribute to susceptibility for COPD.

DAMPs; haplotype association mapping; dsDNA release; *ELAC2*; *PPT1*

CHRONIC OBSTRUCTIVE PULMONARY DISEASE (COPD) is a severe and progressive inflammatory lung disease, characterized by both chronic bronchitis and emphysema. COPD is mainly

caused by chronic exposure to noxious gases and particles, including cigarette smoke (CS) (6). Nevertheless, ~30% of COPD patients are a never smoker, indicating that also other factors, including biomass smoke exposure, air pollution, prenatal factors, and genetics, contribute to the inception of COPD (37). Moreover, only 20% of the smoking population develops COPD (45), further indicating that genetic susceptibility is important for the onset of COPD. To date, treatment options for COPD are limited, and current treatments are aimed at reducing the severity of symptoms and reducing the number and severity of exacerbations, without addressing the underlying cause of the disease. Therefore, a more detailed understanding of disease pathophysiology is imperative for the identification of novel treatment options.

During the early stages of COPD, airway inflammation is characterized by extensive activation of the innate immune system, while at later stages of the disease the adaptive immune system is also involved (12). A mechanism triggering activation of innate immune responses is the release of damage-associated molecular patterns (DAMPs). DAMPs are a heterogeneous group of molecules that possess a wide variety of functions under physiological conditions (5). On cellular damage and necrosis, DAMPs are released from the cells and act as endogenous danger molecules that alarm and activate the innate immune system (31). Although DAMPs are a heterogeneous group of molecules, they all have in common that, on release from damaged or necrotic cells, they can activate one or several pattern recognition receptors (PRRs), including toll-like receptors and the receptor for advanced glycation end products (RAGE) (47). The activation of PRRs leads to activation of inflammatory pathways, including nuclear factor- κ B, inducing the release of inflammatory cytokines, including IL-6, IL-8, and TNF- α (44). The release of these cytokines, together with the direct effect of some DAMPs, leads to the attraction of several innate immune cells, including neutrophils and inflammatory monocytes, to the site of tissue damage (47). Recently, our laboratory postulated that DAMPs may play a crucial role in the pathophysiology of COPD, as inhaled CS induces damage to lung resident cells, such as the airway epithelium, leading to the release of DAMPs and subsequent production of proinflammatory cytokines, which causes neutrophilic airway

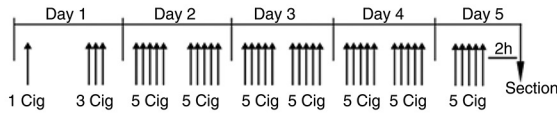
Address for reprint requests and other correspondence: S. D. Pouwels, Dept. of Pathology and Medical Biology, UMCG, Hanzeplein 1, Groningen 9713 GZ, The Netherlands (e-mail: s.d.pouwels@umcg.nl).

inflammation (47). Indeed, several DAMPs are increased in COPD patients compared with both smoking and nonsmoking controls, including heat shock protein (HSP) 60/70 in serum (47), S100A8/A9 in bronchoalveolar lavage (BAL) fluid (40), the human cathelicidin peptide LL-37 in sputum and BAL fluid (27, 59), and high-mobility group box 1 (HMGB1) in BAL fluid, sputum, serum, and epithelial lining fluid (14, 25, 28). Furthermore, the gene encoding RAGE, *AGER*, has been identified as a susceptibility gene for lung function decline and

COPD development (7, 8, 51). Together, these data indicate that DAMPs may play a pivotal role in the pathophysiology of COPD.

Genetic susceptibility for COPD is complex and is regulated by many different genes (42). To increase the knowledge about the genetics of COPD, it is important to study the pathways that lead to emphysema and neutrophilic airway inflammation separately. Some studies have been performed investigating the genetics of emphysema (8). In contrast, limited data are

A Subchronic smoke exposure model



Storage of:
Broncho-alveolar lavage fluid
Lung tissue
Serum
Skeletal muscle

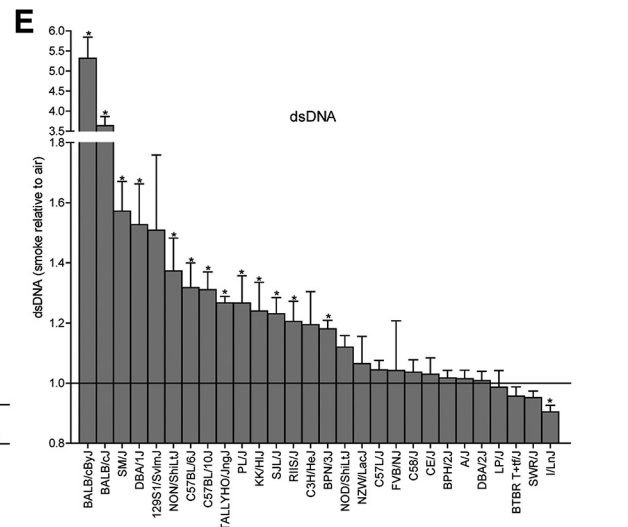
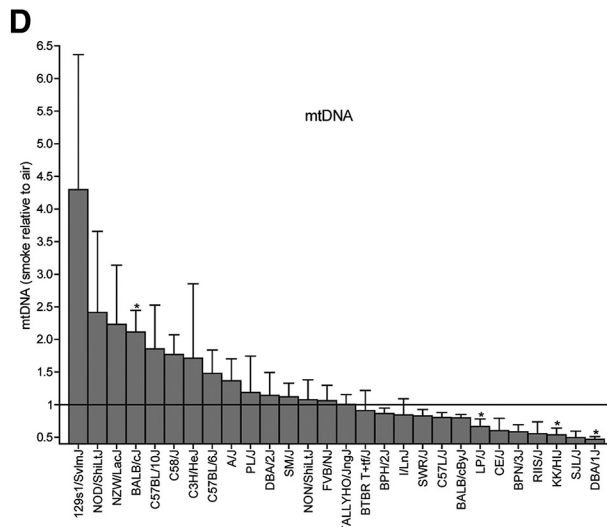
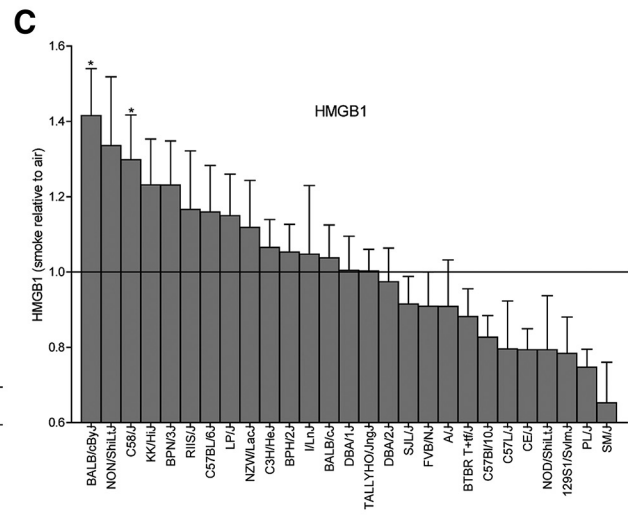
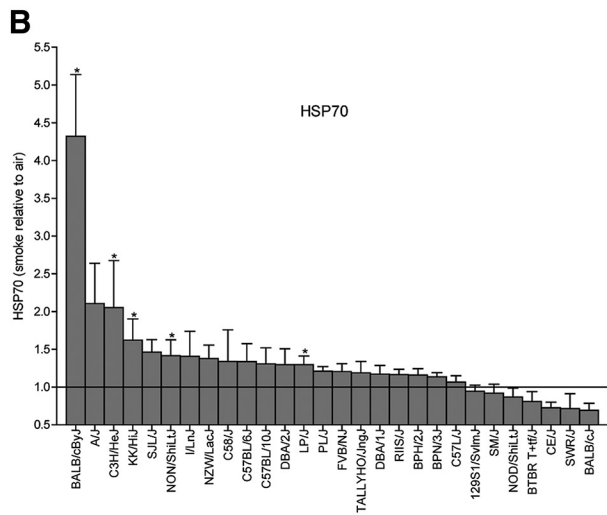


Fig. 1. Cigarette smoke-induced damage-associated molecular pattern (DAMP) release in bronchoalveolar lavage (BAL) fluid from 28 inbred mouse strains. A: schematic representation of the experimental setup. Mice were exposed to cigarette smoke or control air for 5 consecutive days. For each cigarette smoke exposure session, 1, 3, or 5 cigarettes (Cig) were used, with 2 exposures/day, except on the 5th day, when only 1 exposure session was performed. Mice were euthanized 2 h after the final exposure on the 5th day. BAL fluid, lung tissue, serum, and skeletal muscle samples were isolated, aliquoted, and stored at -80°C until further use. The cigarette smoke-induced levels of heat shock protein 70 (HSP70; B), high-mobility group box 1 (HMGB1; C), mitochondrial (mt) DNA (D), and double-stranded (ds) DNA (E) in BAL fluid of 28 inbred mouse strains are shown. Values are average and SE of the mean of the ratio of smoke-exposed mice ($n = 8$) to the average of air-exposed mice ($n = 8$). Significance between DAMP levels of mice exposed to CS and mice exposed to air was tested using a Mann Whitney *U*-test. * $P < 0.05$.

available investigating the genetics underlying the susceptibility to neutrophilic airway inflammation. Previously, it was found that neutrophilic airway inflammation already occurs on short-term smoke exposure in susceptible mice and humans (43, 56). We recently performed a genetic screen using 28 inbred mouse strains and identified several susceptibility genes for short-term CS-induced neutrophilic airway inflammation in mice using haplotype association mapping (HAM) (46). This approach has previously been shown to be effective for identifying susceptibility genes for acrolein-, chlorine-, or ventilator-induced acute lung injury (33–36). In a separate study using a subset of mice from this screen, we found that mice susceptible for CS-induced neutrophilic airway inflammation display a different DAMP-release profile in BAL fluid compared with mice that are not susceptible to CS-induced neutrophilic airway inflammation (48). Therefore, we hypothesize that an increased susceptibility for CS-induced DAMP release leads to increased CS-induced neutrophilic airway inflammation. Here, we further explored the effect of genetic susceptibility for neutrophilic airway inflammation on DAMP release and studied which genes regulate CS-induced DAMP release, using *in vitro*, *in vivo*, and *in silico* approaches.

In these studies, we have identified two novel candidate genes for the susceptibility to CS-induced DAMP release and show that these genes contribute to the susceptibility for CS-induced airway inflammation, indicating that the tendency for CS-induced DAMP release may contribute to the susceptibility for COPD.

MATERIALS AND METHODS

Experimental design. This study was performed after approval from the Institutional Animal Care and Use Committee of the University of Groningen. For this study, 28 inbred mouse strains (females, age 8–10 wk; $n = 16$ mice/strain, The Jackson Laboratory, Bar Harbor, ME) were exposed to gaseous-phase CS from Kentucky 3R4F research reference cigarettes (Tobacco Research Institute, University of Kentucky, Lexington, KY) or air as control, as described previously (50). In short, filters were removed from each cigarette before being smoked in 5 min at a rate of 5 l/h and mixed with ambient air at a rate of 60 l/h using whole body exposure in 6-liter Perspex boxes. Female mice ($n = 8$ /group) were exposed to CS of one to five cigarettes or filtered air ($n = 8$ /group) for 5 consecutive days, with two exposures/day (50). Mice were euthanized 2 h after the final exposure session (Fig. 1A). Lung tissue (four individual lobes) and BAL fluid (1 ml, 100- μ l aliquots) were collected and stored at -80°C until further use. BAL neutrophil counts were analyzed using differential cell counts performed with cytospin smears using the May-Grünwald Giemsa method (2).

HAM analysis. HAM was performed for the log-transformed BAL double-stranded DNA (dsDNA) levels, as described before, using the efficient mixed-model association (EMMA), which conducts tests for association on single nucleotide polymorphisms (SNPs) with two alleles and is corrected for confounding from population structure and genetic relatedness (4, 29, 50). The analysis was performed using a high-density SNP map of 4×10^6 SNPs. SNP names and locations were based on mouse genome build 38. The publicly available R-package implementation of EMMA (available at <http://mouse.cs.ucla.edu/emma/>) was used. The standard significance threshold of $-\log(P) = 5$ was used (4, 30).

DAMP measurements and gene expression analysis. DAMPs were measured in cell-free BAL fluid using ELISA for HSP70 (Human/Mouse/Rat Total HSP70/HSPA1A DuoSet, R&D Systems, Minneapolis, MN) and HMGB1 (HMGB1 Detection Kit, Chondrex, Redmond,

WA), using the Quant-iT PicoGreen dsDNA Assay Kit for dsDNA (Invitrogen, Carlsbad, CA) and quantitative real-time-PCR using iTaq Universal SYBR Green Supermix (Bio-Rad, Richmond, CA) for mitochondrial DNA (mtDNA), as described before (60). Primers for mouse cytochrome-*c* oxidase III (*Mtco3*), 5'-ACGAAACCACATA-AATCAAGCC-3' (forward) and 5'-TAGCCATGAAGAATGTAG-AACC-3' (reverse) were synthesized and purchased from Invitrogen. Standard curves for mtRNA were prepared using purified mtDNA as targets.

For mRNA expression analyses, RNA was isolated from lung tissue homogenate using Trizol (Invitrogen). Further purification of RNA was performed using RNeasy Plus Mini Kit (Qiagen, Valencia, CA), and any remaining DNA was removed using the RNase-Free DNase Set (Qiagen, Valencia, CA). The total amount of RNA was quantified using a Nanodrop-1000 (Nanodrop Technologies, Wilmington, DE). Afterwards, cDNA synthesis was performed according to the manufacturer's protocol using the iScript cDNA synthesis kit (Bio-Rad, Richmond, CA). Quantification of cDNA targets was performed with the TaqMan technology using the ABI 7900HT Sequence Detection System (Applied Biosystems, Foster City, CA). All reactions were run in duplicate. Normalization was performed using multiple housekeeping genes (HKG), which were included on each plate (*B2m*, *Ipo8*, *Pgk1*). The level and stability of expression of the HKGs were determined in all samples, and the most appropriate set of HKGs was chosen (*Ipo8* and *Pgk1* in all cases in this paper) using NormFinder (1). Gene expression analyses were performed using commercially available primer/probe sets specific for target genes (Invitrogen Life Technologies, Carlsbad, CA): *Aox311* (Mm01255397_m1), *Arhgap44* (Mm00812556_m1), *Arhgef11* (Mm01219448_m1), *Cap1* (Mm00482950_m1), *Cflar* (Mm01255578_m1), *Dscam11* (Mm01174253_m1), *Elac2* (Mm01332348_m1), *Enox1* (Mm01315253_m1), *Myocd* (Mm00455051_m1), *Ppt1* (Mm00477078_m1), and *Trip11* (Mm01336257_m1). Genotypes were determined using the publicly available Jackson Laboratory mouse SNP database (available at <http://www.informatics.jax.org/snp>).

Cell culture and CS extract stimulation. The human bronchial epithelial cell-lines, 16HBE (kindly provided by Dr. D. C. Gruenert; University of California, San Francisco, CA) and Beas2B (ATCC, CRL-9609) and the adenocarcinoma human alveolar cell-line A549 were cultured in RPMI-1640 supplemented with 10% fetal calf serum (Biowhittaker, Verviers, Belgium), 100 U/ml penicillin, and 100 mg/ml streptomycin. Before usage, cells were grown to confluence and serum-deprived overnight. CS extract (CSE) was prepared using two Kentucky 3R4F research-reference filtered cigarettes and a Watson Marlow 603S smoking pump at a rate of 8 l/h (Watson-Marlow, Delden, The Netherlands). Before use, filters were cut from both of the cigarettes. The gaseous-phase CS of two cigarettes was led through 25 ml of RPMI-1640 medium supplemented with 100 U/ml penicillin and 100 mg/ml streptomycin, and this solution was set at 100% CSE.

Small interfering RNA transfection. Downregulation of candidate genes was performed with commercially available small interfering

Table 1. Characteristics of the young, healthy individuals susceptible or nonsusceptible for the development of COPD

	Young Nonsusceptible	Young Susceptible
<i>n</i>	18	17
Age, yr	25 ± 8.33	29.35 ± 8.50
Pack years	4 ± 6.77	4.2 ± 3.52
Sex, male (%)	16 (88.89)	11 (64.7)
FEV ₁ , %predicted	103.65 ± 7.52	100.74 ± 8.40

Values are means ± SD, unless stated otherwise; *n*, no. of subjects. FEV₁, forced expiratory volume in 1 s. Differences in variables before and after treatment were analyzed using a two-sided, paired, Student's *t*-test.

RNA (siRNA) assays, according to the manufacturer's protocol (MISSION endoribonuclease-prepared siRNA for *PPT1*, *ELAC2*, *ENOX1*, and *ARHGEF11*; Sigma-Aldrich, St. Louis, MO), using RNAiMAX lipofectamine as a transfection reagent (Invitrogen).

Cells were exposed to various concentrations of CSE for 4 h before being incubated with serum- and CSE-free medium for 16 h. The levels of dsDNA and RNA were determined in cell-free supernatant using the Quant-iT Pico- and Ribo-Green dsDNA Assay Kits,

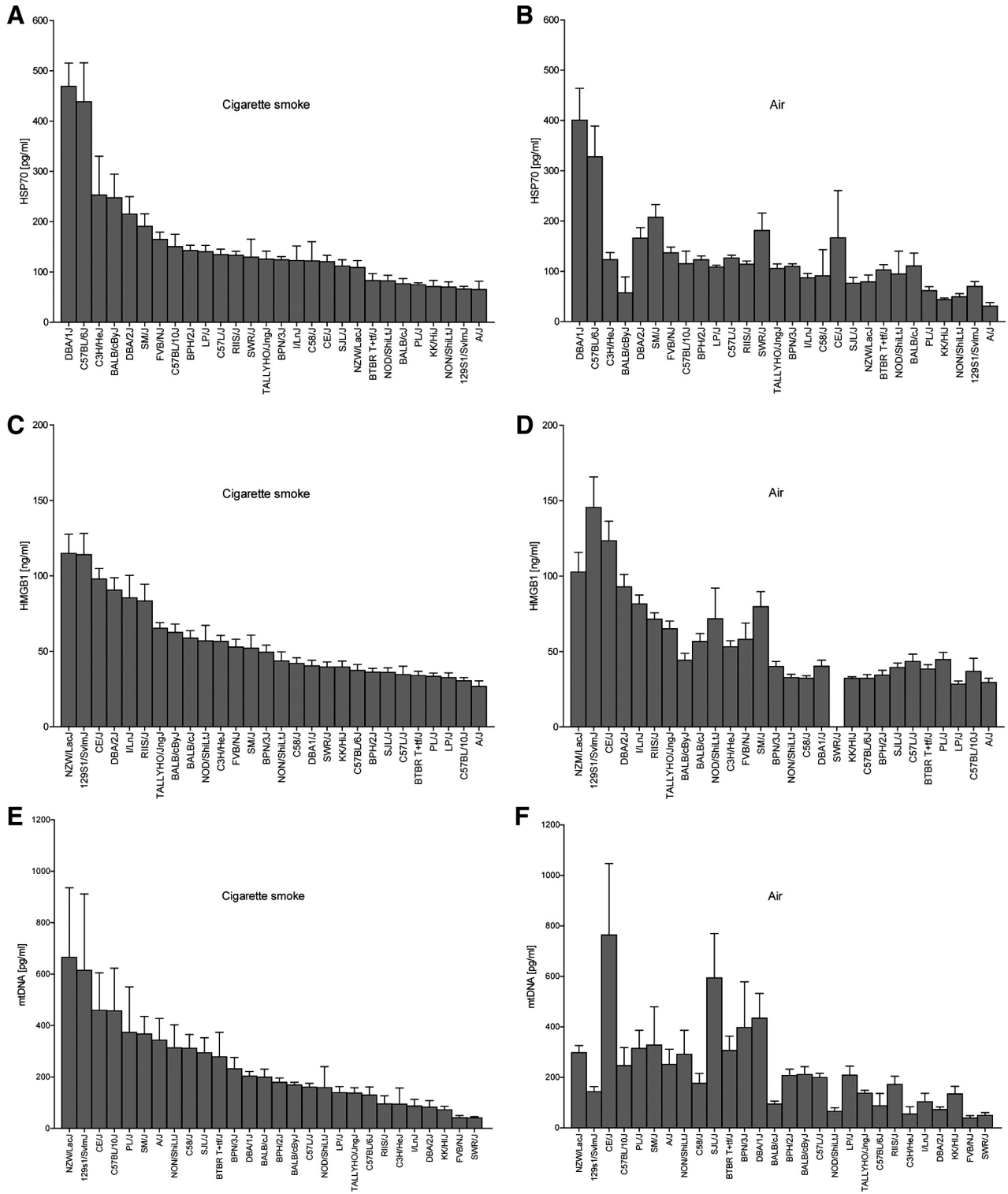


Fig. 2. The levels of damage-associated molecular patterns (DAMPs) in bronchoalveolar lavage (BAL) fluid from 28 inbred mouse strains on cigarette smoke (CS; A, C, and E) or air exposure (B, D, and F). The levels of heat shock protein 70 (HSP70; A and B), high-mobility group box 1 (HMGB1; C and D), and mitochondrial (mt) DNA (E and F) in BAL fluid of 28 mouse strains on CS or air exposure are shown. Values are average and SE of the mean of 8 mice/group.

respectively (Invitrogen). The percentage of viable, apoptotic, and necrotic cells was determined using an annexin V (Immunotools, Friesoythe, Germany) and propidium iodide (Sigma-Aldrich) staining for flow cytometry.

Human gene expression analysis. The study was approved by the Medical Ethics Committee of the University Medical Center Groningen (UMCG), and all subjects gave their written, informed consent. The study protocol was consistent with the Research Code of the UMCG (<https://www.umcg.nl/EN/RESEARCH/RESEARCHERS/GENERAL/RESEARCHCODE/paginas/default.aspx>) and national ethical and professional guidelines (<https://www.federa.org>). Young, healthy individuals were classified as susceptible when the prevalence of COPD in smoking first- or second-degree relatives older than 40 yr met the following criteria, two of two, two of three, three of three, three of four, or four of four smoking family members had developed COPD, and were classified as nonsusceptible when none of the smoking first- or second-degree relatives who were at least 40 yr of age (at least two should be identified) had been diagnosed with COPD. Subjects were included in the study if they had smoked only occasionally and were able to start or stop smoking on demand. Bronchial brushings for gene expression profiling were performed after smoking three cigarettes within 3 h and after a smoking cessation period of at least 48 h ($n = 35$). The characteristics of the study participants are summarized in Table 1. The change in bronchial epithelial gene expression before and after smoking of three cigarettes was determined using a linear regression analysis, with time defined as a categorical variable with two levels (1 = baseline, 2 = after smoking of three cigarettes), adjusted for age and sex as possible confounding variables. Ge_{ij} represents the log₂ gene expression value for a gene in *sample i* from *patient j*, ϵ_{ij} represents the error that is assumed to be normally distributed:

$$Ge_{ij} = \beta_0 + \beta_1 X_{Age-i} + \beta_2 X_{Sex-i} + \beta_3 X_{Time-i}$$

where β_0 is the constant (offset) term and $\beta_1 X_{Age-i}$, $\beta_2 X_{Sex-i}$, and $\beta_3 X_{Time-i}$ are the independent variables. The change in bronchial epithelial gene expression before and after smoking of three cigarettes was determined between young occasional smokers either susceptible or nonsusceptible for COPD. This analysis was performed using a linear mixed-effects model with time defined as a categorical variable with two levels (1 = baseline, 2 = after smoking of three cigarettes) adjusted for age and sex. Ge_{ij} represents the log₂ gene expression

value for a gene in *sample i* from *patient j*, ϵ_{ij} represents the error that is assumed to be normally distributed, and α_j represents the patient random effect:

$$Ge_{ij} = \beta_0 + \beta_1 X_{Age-i} + \beta_2 X_{Sex-i} + \beta_3 X_{susceptibility_for_COPD-i} + \beta_4 X_{Time-i} + \beta_3 X_{susceptibility_for_COPD-i} : \beta_4 X_{Time-i}$$

Statistical analysis. All data are shown as means \pm SE, except for mRNA expression data, which is shown as box-whisker plots indicating the mean \pm interquartile range, with the whiskers indicating the highest and lowest data point. A Mann-Whitney *U*-test was used to test for differences between groups. To test for differences in basal gene expression between mouse strains, a one-way ANOVA with Turkey's multiple-comparison correction was performed. Normality in distribution of BAL dsDNA levels was tested using the Shapiro-Wilk normality test, with a significance threshold of $P < 0.05$. Correlations were determined using a linear regression analysis, with a significance threshold of P value of <0.001 .

RESULTS

Susceptibility for CS-induced DAMP release is genetically determined. To investigate whether susceptibility to CS-induced neutrophilia can be explained by differences in DAMP release, we made use of a previously established data set from a genetic screen where 28 different inbred mouse strains were exposed to CS for 5 consecutive days (Fig. 1A) (46). We measured the levels of four well-known DAMPs, HSP70, HMGB1, mtDNA, and dsDNA, in BAL fluid on air and CS exposure (Fig. 1, B–E). While basal (air-exposed) levels of all DAMPs showed some variation between strains (Fig. 2), the CS-induced DAMP levels varied more extensively between strains for all four DAMPs studied. This was most pronounced for dsDNA, in which CS exposure induced a 6-fold induction in BAL fluid of BALB/cByJ, the most susceptible strain for neutrophilic airway inflammation, and a 0.1-fold decrease in the nonsusceptible I/LnJ strain, while its levels did not strongly differ between the strains at baseline (Fig. 3).

Next, we investigated whether the number of neutrophils in BAL fluid of 28 mouse strains after CS exposure correlated

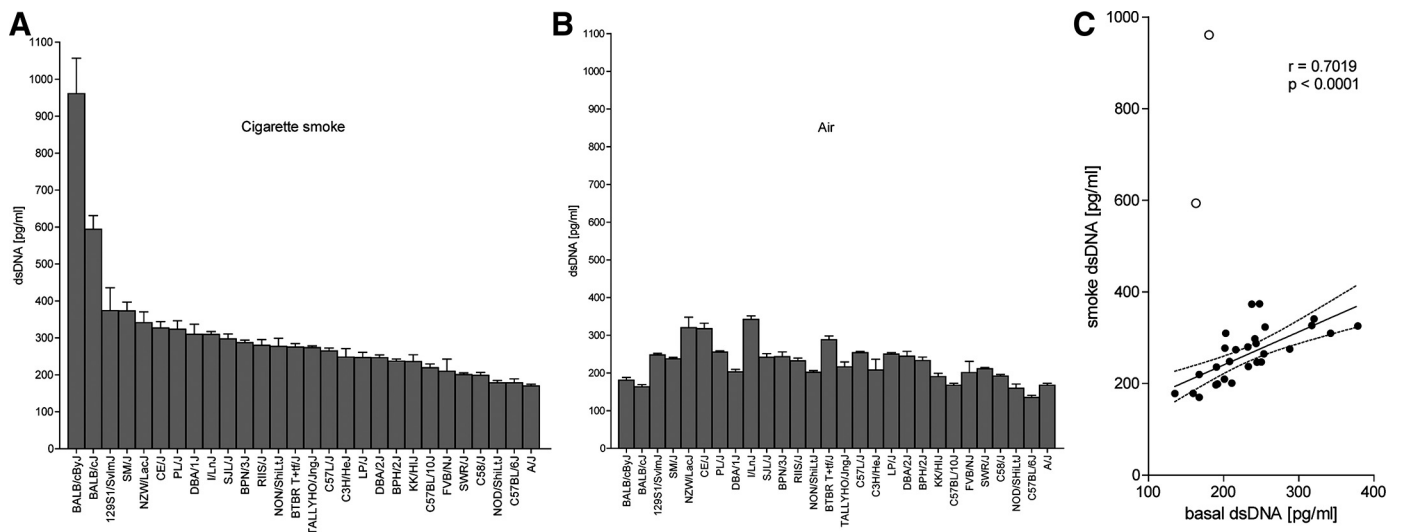


Fig. 3. The levels of double-stranded (ds) DNA in 28 inbred mouse strains on cigarette smoke (CS) or air exposure. The levels of dsDNA in bronchoalveolar lavage (BAL) fluid of 28 mouse strains on CS (A) or air exposure (B) are shown. Values are average and SE of the mean of 8 mice/group. C: the association between the dsDNA levels in BAL fluid of 28 mouse strains on CS exposure and air exposure. Correlation was tested using a linear regression analysis ($r = 0.7019$, $P < 0.0001$).

with the levels of DAMPs in the BAL fluid after CS exposure. A strong and significant correlation between dsDNA and airway neutrophilia ($r = 0.8077$, $P \leq 0.0001$) was found (Fig. 4A), but not for HMGB1 ($r = 0.061$, $P = 0.349$), HSP70 ($r = 0.0227$, $P = 0.7276$), or mtDNA ($r = 0.0177$, $P = 0.7886$) (Fig. 4, B–D).

These data show that CS-induced DAMP release varies largely between different mouse strains, indicating the contribution of a genetic component to the magnitude of this response. Furthermore, of the four DAMPs analyzed, dsDNA showed the largest variation between strains and showed the strongest correlation with CS-induced airway neutrophilia, making dsDNA the most relevant for further investigation.

Identification of susceptibility genes for basal and CS-induced BAL dsDNA levels in mice. To investigate which genes are associated with basal dsDNA levels in mice, a HAM analysis was performed using the EMMA (33, 46) software on the log-transformed dsDNA levels in 28 different inbred mouse strains. BAL dsDNA levels in air-exposed mice strongly correlated with CS-induced dsDNA levels after removal of the outliers BALB/c and BALB/cByJ ($r = 0.7019$, $P \leq 0.0001$), indicating that dsDNA release is, at least in part, regulated by mechanisms that operate, irrespective of CS exposure (Fig. 3C). Therefore, we first analyzed BAL dsDNA levels in both mice groups, using CS exposure as a covariate for the analysis. This analysis identified 99 SNPs associated with dsDNA levels with genome-wide significance (Table 2), of which 49 were located within a gene and had less than six mouse strains with

missing data (Table 3). The genes significantly associated with dsDNA release consist of *Aox3ll* (2 SNPs) and *Cflar* (1 SNP) on *chromosome 1*; *Arhgef11* (3 SNPs) on *chromosome 3*; *Ppt1* (1 SNP) and *Cap1* (4 SNPs) on *chromosome 4*; *Elac2* (2 SNPs), *Arhgap44* (26 SNPs), and *Myocd* (7 SNPs) on *chromosome 11*; and *Trip11* on *chromosome 12* (3 SNPs) (Fig. 5).

We next analyzed which SNPs were specifically associated with the CS-induced dsDNA levels, using the log-transformed BAL dsDNA levels of smoke-exposed mice only as input for the analysis. With the use of all 28 mouse strains available in the EMMA database, no significant hits were found. This may be caused by the extreme effect of CS exposure on BAL dsDNA levels in the BALB/cJ and the BALB/cByJ strains, acting as outliers in the analysis. Therefore, these strains were removed from the HAM analysis for CS-induced dsDNA release. This second analysis identified 48 significant SNPs specifically associated with CS-induced dsDNA levels (Table 4), of which 18 were located within a gene and had less than 6 mouse strains with missing data (Table 5). The genes significantly associated with CS-induced dsDNA release are *Ppt1* (1 SNP) and *Cap1* (1 SNP) on *chromosome 4*; *Dscaml1* (1 SNP) on *chromosome 9*; *Myocd* (6 SNPs) on *chromosome 11*; and *Enox1* on *chromosome 14* (9 SNPs) (Fig. 6).

Three of the genes associated with CS-induced dsDNA levels, *Ppt1*, *Cap1*, and *Myocd*, were also associated with the basal dsDNA levels in the analysis corrected for CS exposure status, indicating that only two genes, *Dscaml1* and

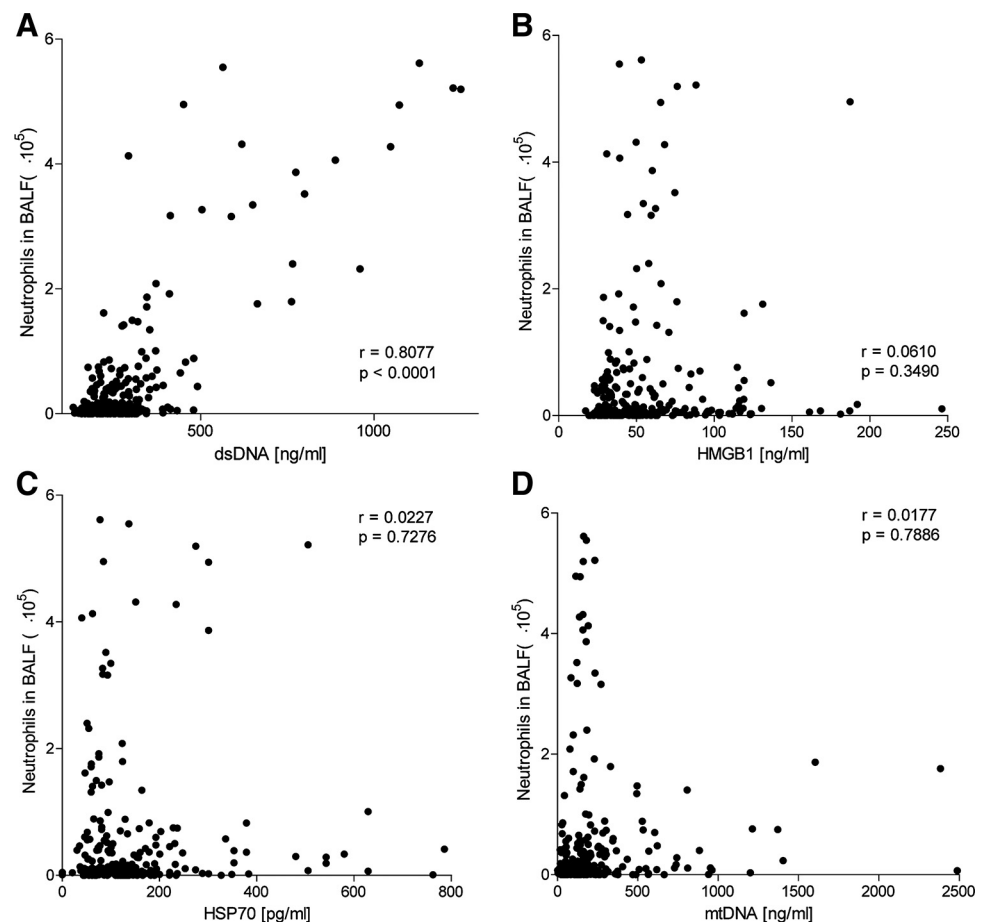


Fig. 4. Correlation between cigarette smoke-induced damage-associated molecular pattern (DAMP) release and neutrophil count in bronchoalveolar lavage (BAL) fluid. The correlation between the number of neutrophils in BAL fluid of cigarette smoke-exposed mice and the levels of double-stranded (ds) DNA (A), high-mobility group box 1 (HMGB1; B), heat shock protein 70 (HSP70; C), and mitochondrial (mt) DNA (D) in BAL fluid on exposure to cigarette smoke for 5 days is shown. The levels of dsDNA show a significant positive linear correlation with neutrophilic infiltrate ($P < 0.0001$, $r = 0.8077$), while the levels of HMGB1 ($P = 0.3490$, $r = 0.0610$), HSP70 ($P = 0.7276$, $r = 0.0227$), and mtDNA ($P = 0.7886$, $r = 0.0177$) do not show a significant correlation with neutrophilic infiltration.

Table 2. Single nucleotide polymorphisms significantly associated with bronchoalveolar lavage double-stranded DNA levels after short-term cigarette smoke exposure in cigarette smoke- and air-exposed mice

Chromosome No.	P Value	Position	Rsid	No. Major Alleles	No. Minor Alleles	No. Missing Alleles	Beta	Gene
1	1.133E-06	58359650	NES16379965	10	15	3	-0.153	<i>Aox3ll</i>
1	5.456E-06	58360789	NES16379942	10	14	4	-0.147	<i>Aox3ll</i>
1	7.659E-06	58805222	NES12804923	8	15	5	-0.156	<i>Cflar</i>
1	7.364E-06	59780091	mm37-1-59780091	15	12	1	-0.124	
3	9.810E-06	58655690	NES12922997	5	15	8	-0.181	<i>Clrn1</i>
3	6.272E-06	87439679	NES14672658	14	14	0	-0.142	<i>Arhgef11</i>
3	6.272E-06	87442284	NES14672597	14	14	0	-0.142	<i>Arhgef11</i>
3	5.605E-06	87487048	mm37-3-87487048	13	14	1	-0.147	<i>Arhgef11</i>
4	5.357E-06	3136046	NES08672116	6	7	15	-0.194	
4	5.357E-06	3136100	NES08672117	6	7	15	-0.194	
4	1.338E-06	122526998	NES09192855	16	9	3	0.149	<i>Ppt1</i>
4	2.579E-06	122551421	NES09192317	17	9	2	0.142	<i>Cap1</i>
4	6.625E-06	122550824	NES09192312	10	16	2	-0.138	<i>Cap1</i>
4	6.625E-06	122550987	NES09192313	10	16	2	-0.138	<i>Cap1</i>
4	6.625E-06	122551398	NES09192316	10	16	2	-0.138	<i>Cap1</i>
4	1.858E-06	122612792	NES09190609	15	10	3	0.144	
4	4.319E-06	122607260	NES09190752	11	14	3	-0.144	
4	6.485E-06	123538006	mm37-4-123538006	17	11	0	0.142	
4	3.506E-06	123571200	NES09195959	16	10	2	0.137	
4	1.701E-06	123635445	NES09194053	12	14	2	-0.146	
4	1.858E-06	123635179	NES09194049	15	10	3	0.144	
4	1.858E-06	123636696	NES09194072	15	10	3	0.144	
4	1.701E-06	123671465	NES09192986	12	14	2	-0.146	
4	1.701E-06	123671910	NES09192992	12	14	2	-0.146	
4	1.701E-06	123672979	NES09192925	12	14	2	-0.146	
4	1.858E-06	123670557	NES09193039	15	10	3	0.144	
4	1.858E-06	123671493	NES09192987	15	10	3	0.144	
4	1.858E-06	123671697	NES09192991	15	10	3	0.144	
4	1.858E-06	123671952	NES09192994	15	10	3	0.144	
4	1.858E-06	123672236	NES09192963	15	10	3	0.144	
4	1.858E-06	123672264	NES09192964	15	10	3	0.144	
8	3.600E-06	7946277	NES14109173	8	19	1	-0.155	
8	3.600E-06	7948439	NES14109038	8	19	1	-0.155	
8	3.600E-06	7949088	NES14109046	8	19	1	-0.155	
8	3.600E-06	7955394	NES14108974	8	19	1	-0.155	
8	3.600E-06	7955590	NES14108977	8	19	1	-0.155	
8	3.600E-06	7957841	NES14108946	8	19	1	-0.155	
8	3.600E-06	7961296	NES14108824	8	19	1	-0.155	
8	3.600E-06	7963293	NES14108855	8	19	1	-0.155	
8	3.600E-06	7965049	NES14108720	8	19	1	-0.155	
8	3.600E-06	7965252	NES14108722	8	19	1	-0.155	
8	3.600E-06	7965725	NES14108727	8	19	1	-0.155	
8	3.600E-06	7979810	NES14108369	8	19	1	-0.155	
8	3.600E-06	7979862	NES14108371	8	19	1	-0.155	
8	3.600E-06	7980132	NES14108373	8	19	1	-0.155	
8	3.600E-06	7980284	NES14108374	8	19	1	-0.155	
8	3.600E-06	7981043	NES14108386	8	19	1	-0.155	
8	3.600E-06	7981992	NES14108330	8	19	1	-0.155	
8	3.600E-06	7982713	NES14108312	8	19	1	-0.155	
8	3.600E-06	7982896	NES14108313	8	19	1	-0.155	
8	3.600E-06	7982996	NES14108315	8	19	1	-0.155	
8	3.600E-06	7983074	NES14108318	8	19	1	-0.155	
8	3.600E-06	7983620	NES14108323	8	19	1	-0.155	
8	3.600E-06	7984300	NES14108261	8	19	1	-0.155	
8	3.600E-06	7986873	NES14108209	8	19	1	-0.155	
8	3.600E-06	7987232	NES14108214	8	19	1	-0.155	
11	2.650E-07	64800867	NES08496202	11	14	3	-0.144	<i>Elac2</i>
11	2.650E-07	64801842	NES08496212	11	14	3	-0.144	<i>Elac2</i>
11	2.280E-06	64764572	mm37-11-64764572	6	21	1	-0.163	
11	1.872E-06	64921523	NES08494443	6	21	1	-0.160	<i>Arhgap44</i>
11	1.872E-06	64924716	NES08494384	6	21	1	-0.160	<i>Arhgap44</i>
11	8.613E-06	64910882	NES08494687	6	19	3	-0.151	<i>Arhgap44</i>
11	8.613E-06	64922067	NES08494457	6	19	3	-0.151	<i>Arhgap44</i>
11	8.613E-06	64924352	NES08494381	6	19	3	-0.151	<i>Arhgap44</i>
11	8.613E-06	64929534	NES08494314	6	19	3	-0.151	<i>Arhgap44</i>
11	8.613E-06	64930953	NES08494276	6	19	3	-0.151	<i>Arhgap44</i>
11	8.613E-06	64931187	NES08494263	6	19	3	-0.151	<i>Arhgap44</i>

Continued

Table 2.—Continued

Chromosome No.	P Value	Position	Rsid	No. Major Alleles	No. Minor Alleles	No. Missing Alleles	Beta	Gene
11	3.637E-07	64976888	mm37-11-64976888	6	20	2	-0.153	<i>Arhgap44</i>
11	1.430E-06	64952961	NES08493948	6	22	0	-0.162	<i>Arhgap44</i>
11	1.430E-06	64953373	mm37-11-64953373	6	22	0	-0.162	<i>Arhgap44</i>
11	1.430E-06	64973258	mm37-11-64973258	6	22	0	-0.162	<i>Arhgap44</i>
11	1.430E-06	64977356	mm37-11-64977356	6	22	0	-0.162	<i>Arhgap44</i>
11	1.872E-06	64948946	NES08493991	6	21	1	-0.160	<i>Arhgap44</i>
11	1.872E-06	64949028	NES08493992	6	21	1	-0.160	<i>Arhgap44</i>
11	6.787E-06	64966804	NES08493729	6	20	2	-0.154	<i>Arhgap44</i>
11	8.613E-06	64947351	NES08494044	6	19	3	-0.151	<i>Arhgap44</i>
11	8.613E-06	64949090	NES08493994	6	19	3	-0.151	<i>Arhgap44</i>
11	8.613E-06	64949443	NES08493986	6	19	3	-0.151	<i>Arhgap44</i>
11	8.613E-06	64955529	NES08493916	6	19	3	-0.151	<i>Arhgap44</i>
11	8.613E-06	64966470	NES08493761	6	19	3	-0.151	<i>Arhgap44</i>
11	8.613E-06	64967419	NES08493710	6	19	3	-0.151	<i>Arhgap44</i>
11	8.613E-06	64967871	NES08493715	6	19	3	-0.151	<i>Arhgap44</i>
11	8.613E-06	64968072	NES08493716	6	19	3	-0.151	<i>Arhgap44</i>
11	8.613E-06	64968132	NES08493717	6	19	3	-0.151	<i>Arhgap44</i>
11	8.613E-06	64968261	NES08493718	6	19	3	-0.151	<i>Arhgap44</i>
11	1.780E-09	64999358	NES08493493	9	15	4	-0.150	<i>Myocd</i>
11	1.430E-06	64990379	mm37-11-64990379	6	22	0	-0.162	<i>Myocd</i>
11	3.781E-06	65009295	NES08493388	10	17	1	-0.133	<i>Myocd</i>
11	3.781E-06	65016012	NES08493236	10	17	1	-0.133	<i>Myocd</i>
11	5.452E-06	65014320	mm37-11-65014320	10	17	1	-0.131	<i>Myocd</i>
11	6.920E-06	65014221	mm37-11-65014221	10	18	0	-0.127	<i>Myocd</i>
11	6.920E-06	65028777	mm37-11-65028777	10	18	0	-0.127	<i>Myocd</i>
12	3.750E-06	21839677	NES17527922	12	2	14	-0.255	<i>Ak020054</i>
12	3.750E-06	23095234	NES17528416	12	2	14	-0.255	
12	6.326E-06	103089429	NES11404685	5	22	1	-0.168	<i>Trip11</i>
12	6.326E-06	103097667	NES11404353	5	22	1	-0.168	<i>Trip11</i>
12	6.326E-06	103098300	NES11404363	5	22	1	-0.168	<i>Trip11</i>
16	2.793E-06	11870630	NES15692525	6	12	10	-0.185	<i>Cpped1</i>
17	1.514E-06	35534387	NES17324125	7	11	10	-0.185	<i>H2-q8</i>

Significance cutoff is set at $-\log(P) \geq 5$. Rsid, reference sequence identification number. Major and minor alleles indicate the number of mouse strains with the most and least abundant allele for the SNP, respectively. Missing alleles indicate the number of mouse strains with missing data for the SNP. SNP names and locations were based on mouse genome build 38.

Enox1, are specifically associated with CS-induced dsDNA release. On inspection of the gene ontology of the 11 genes associated with overall or CS-induced dsDNA release, we did not identify a single pathway in which all genes operate (Table 6). However, several of these genes, i.e., *Cflar*, *Ppt1*, *Cap1*, *Enox1*, and *Elac2*, are involved in apoptosis and DNA damage responses.

Gene expression of candidate genes in lung tissue of mice susceptible or nonsusceptible for CS-induced dsDNA release. SNPs can modify gene function by altering regulation of gene expression at the mRNA or protein level, or by directly altering protein function in case of nonsynonymous coding SNPs. As can be seen in Tables 3 and 5, we did not identify any nonsynonymous coding SNPs in our analysis. Therefore, we compared lung tissue gene expression levels between mouse strains susceptible and nonsusceptible for CS-induced dsDNA release. To this end, two susceptible mouse strains, BALB/cByJ and PL/J, and two nonsusceptible mouse strains, C58/J and A/J, were selected for further analysis. The basal mRNA expression of the 11 candidate genes identified using HAM analysis was determined in lung tissue of these strains (Fig. 7). In all cases, a single haplotype block spanning (part of) the gene was identified, and genotype of a representative SNP within the haplotype block is provided.

The two susceptible mouse strains showed a higher basal expression of *Ppt1* compared with the nonsusceptible mouse

strains, while the expression of *Enox1* was only higher in the susceptible BALB/cByJ strain. In contrast, the expression of *Elac2* was higher in the two nonsusceptible mouse strains. For *Arhgap44*, *Arhgef11*, *Cap1*, and *Trip11*, the expression is the lowest in the nonsusceptible A/J strain but with also low expression in the susceptible BALB/cByJ strain, whereas for *Dscaml1*, *Aox3ll*, and *Myocd*, the highest basal expression was found in the C58/J strain. Finally for *Cflar*, no differences in basal gene expression were shown between the different strains. The overall differences in basal mRNA expression levels between strains were relatively small, and only for *Ppt1* and *Elac2* was an association with genotype found.

We next identified the effect of CS exposure on gene expression of the 11 candidate genes by measuring the mRNA expression in lung tissue of the 2 susceptible and 2 nonsusceptible mouse strains exposed to air or smoke (Fig. 8). Here, CS exposure leads to a decrease in *Arhgef11*, *Elac2*, *Enox1*, and *Trip11* gene expression in at least one of the nonsusceptible mouse strains. This effect was even stronger for *Dscaml1*, where the mRNA expression was not only decreased by CS exposure in the nonsusceptible strains, but also significantly increased by CS in the susceptible mouse strains. In contrast, CS leads to a decrease in *Ppt1* gene expression for both susceptible mouse strains and in *Myocd* gene expression for the susceptible BALB/cByJ strain. For *Aox3ll*, *Arhgap44*, and *Cflar*, hardly any effect of CS exposure on gene expression was shown. Only for *Ppt1* and *Elac2* were the effects of CS

Table 3. Selected single nucleotide polymorphisms significantly associated with bronchoalveolar lavage double-stranded DNA levels after short-term cigarette smoke exposure in cigarette smoke- and air-exposed mice

Chromosome No.	P Value	Position	Rsid	No. Major Alleles	No. Minor Alleles	No. Missing Alleles	Beta	Function Class	BALB/cByJ	PL/J	C58/J	A/J	Gene
1	1.133E-06	58359650	NES16379965	10	15	3	-0.153	Int	C	C	T	T	<i>Aox3l1</i>
1	5.456E-06	58360789	NES16379942	10	14	4	-0.147	Int	C	C	G	G	<i>Aox3l1</i>
1	7.659E-06	58805222	NES12804923	8	15	5	-0.156	Int	T	T	C	C	<i>Cflar</i>
3	6.272E-06	87439679	NES14672658	14	14	0	-0.142	Int	T	T	C	C	<i>Arhgef11</i>
3	6.272E-06	87442284	NES14672597	14	14	0	-0.142	Int	T	T	C	C	<i>Arhgef11</i>
3	5.605E-06	87487048	mm37-3-87487048	13	14	1	-0.147	Int	T	T	C	C	<i>Arhgef11</i>
4	5.357E-06	3136046	NES08672116	16	9	3	0.149	uk	uk	uk	uk	uk	<i>Ppt1</i>
4	2.579E-06	122551421	NES09192317	17	9	2	0.142	Int	G	G	G	A	<i>Cap1</i>
4	6.625E-06	122550824	NES09192312	10	16	2	-0.138	Int	G	G	G	T	<i>Cap1</i>
4	6.625E-06	122550987	NES09192313	10	16	2	-0.138	Int	T	T	T	A	<i>Cap1</i>
4	6.625E-06	122551398	NES09192316	10	16	2	-0.138	Int	C	C	C	T	<i>Cap1</i>
11	2.650E-07	64800867	NES08496202	11	14	3	-0.144	Int	C	C	T	T	<i>Elac2</i>
11	2.650E-07	64801842	NES08496212	11	14	3	-0.144	Int	C	C	T	T	<i>Elac2</i>
11	1.872E-06	64921523	NES08494443	6	21	1	-0.160	Int	A	A	C	C	<i>Arhgap44</i>
11	1.872E-06	64924716	NES08494384	6	21	1	-0.160	Int	T	T	G	G	<i>Arhgap44</i>
11	8.613E-06	64910882	NES08494687	6	19	3	-0.151	Int	C	C	A	A	<i>Arhgap44</i>
11	8.613E-06	64922067	NES08494457	6	19	3	-0.151	Int	A	A	G	G	<i>Arhgap44</i>
11	8.613E-06	64924352	NES08494381	6	19	3	-0.151	Int	C	C	T	T	<i>Arhgap44</i>
11	8.613E-06	64929534	NES08494314	6	19	3	-0.151	Int	T	T	C	C	<i>Arhgap44</i>
11	8.613E-06	64930953	NES08494276	6	19	3	-0.151	Int	C	C	T	T	<i>Arhgap44</i>
11	8.613E-06	64931187	NES08494263	6	19	3	-0.151	Int	G	G	A	A	<i>Arhgap44</i>
11	3.637E-07	64976888	mm37-11-64976888	6	20	2	-0.153	uk	C	C	T	T	<i>Arhgap44</i>
11	1.430E-06	64952961	NES08493948	6	22	0	-0.162	Int	C	C	T	T	<i>Arhgap44</i>
11	1.430E-06	64953373	mm37-11-64953373	6	22	0	-0.162	Int	G	G	A	A	<i>Arhgap44</i>
11	1.430E-06	64973258	mm37-11-64973258	6	22	0	-0.162	Int	G	G	A	A	<i>Arhgap44</i>
11	1.430E-06	64977356	mm37-11-64977356	6	22	0	-0.162	uk	C	C	T	T	<i>Arhgap44</i>
11	1.872E-06	64948946	NES08493991	6	21	1	-0.160	Int	C	C	T	T	<i>Arhgap44</i>
11	1.872E-06	64949028	NES08493992	6	21	1	-0.160	Int	C	C	T	T	<i>Arhgap44</i>
11	6.787E-06	64966804	NES08493729	6	20	2	-0.154	Int	G	G	A	A	<i>Arhgap44</i>
11	8.613E-06	64947351	NES08494044	6	19	3	-0.151	Int	T	T	C	C	<i>Arhgap44</i>
11	8.613E-06	64949090	NES08493994	6	19	3	-0.151	Int	A	A	G	G	<i>Arhgap44</i>
11	8.613E-06	64949443	NES08493986	6	19	3	-0.151	Int	C	C	T	T	<i>Arhgap44</i>
11	8.613E-06	64955529	NES08493916	6	19	3	-0.151	Int	A	A	T	T	<i>Arhgap44</i>
11	8.613E-06	64966470	NES08493761	6	19	3	-0.151	Int	A	A	T	T	<i>Arhgap44</i>
11	8.613E-06	64967419	NES08493710	6	19	3	-0.151	Int	G	G	C	C	<i>Arhgap44</i>
11	8.613E-06	64967871	NES08493715	6	19	3	-0.151	Int	G	G	A	A	<i>Arhgap44</i>
11	8.613E-06	64968072	NES08493716	6	19	3	-0.151	Int	A	A	T	T	<i>Arhgap44</i>
11	8.613E-06	64968132	NES08493717	6	19	3	-0.151	Int	G	G	A	A	<i>Arhgap44</i>
11	8.613E-06	64968261	NES08493718	6	19	3	-0.151	Int	C	C	G	G	<i>Arhgap44</i>
11	1.780E-09	64999358	NES08493493	9	15	4	-0.150	Int	T	T	C	C	<i>Myocd</i>
11	1.430E-06	64990379	mm37-11-64990379	6	22	0	-0.162	UTR	A	A	G	G	<i>Myocd</i>
11	3.781E-06	65009295	NES08493388	10	17	1	-0.133	Int	C	C	T	T	<i>Myocd</i>
11	3.781E-06	65016012	NES08493236	10	17	1	-0.133	Int	G	G	A	A	<i>Myocd</i>
11	5.452E-06	65014320	mm37-11-65014320	10	17	1	-0.131	Cs P:227	G	G	C	C	<i>Myocd</i>
11	6.920E-06	65014221	mm37-11-65014221	10	18	0	-0.127	Int	C	C	T	T	<i>Myocd</i>
11	6.920E-06	65028777	mm37-11-65028777	10	18	0	-0.127	Int	A	A	G	G	<i>Myocd</i>
12	6.326E-06	103089429	NES11404685	5	22	1	-0.168	Int	C	C	uk	T	<i>Trip11</i>
12	6.326E-06	103097667	NES11404353	5	22	1	-0.168	Int	G	G	uk	A	<i>Trip11</i>
12	6.326E-06	103098300	NES11404363	5	22	1	-0.168	Int	G	G	uk	A	<i>Trip11</i>

Significant SNPs were located within a gene and had less than six mouse strains with missing data. Significance cutoff is set at $-\log(P) \geq 5$. The number of major and minor alleles indicate the number of mouse strains with the most and least abundant allele for the SNP, respectively, from the 28 mouse strains used in our analyses. Number of missing alleles indicates the number of mouse strains with missing data for the SNP. Function class is intronic (Int), synonymous-codon (Cs) with the amino acid and location, or 3'-untranslated region (UTR). Missing information is noted as unknown (uk). Position is the base pair location of the SNP. SNP names and locations were based on mouse genome build 38.

exposure on gene expression levels in lung tissue in accordance with the identified genotypes.

Together, we found small, yet significant, differences in the basal mRNA expression levels between different strains. However, only for *Ppt1* and *Elac2* were the gene expression levels associated with the genotype of the haplotype block identified in our EMMA analysis, indicating that one of the SNPs present in the haplotype block might function as an expression quantitative trait locus (eQTL). CS exposure induced changes in gene expression of the candidate genes in spe-

cific strains, with the strongest effect on *Dscam11*, which increased in the susceptible strains and decreased in at least one nonsusceptible strain. Furthermore, for *Ppt1*, the decrease in expression was only noted in susceptible mouse strains, while for *Elac2* the CS-induced decrease in gene expression was only noted in nonsusceptible mouse strains. These data indicate that, for these two genes, the effect of CS on their gene expression regulation may contribute to differences in susceptibility for CS-induced dsDNA release in the mouse model.

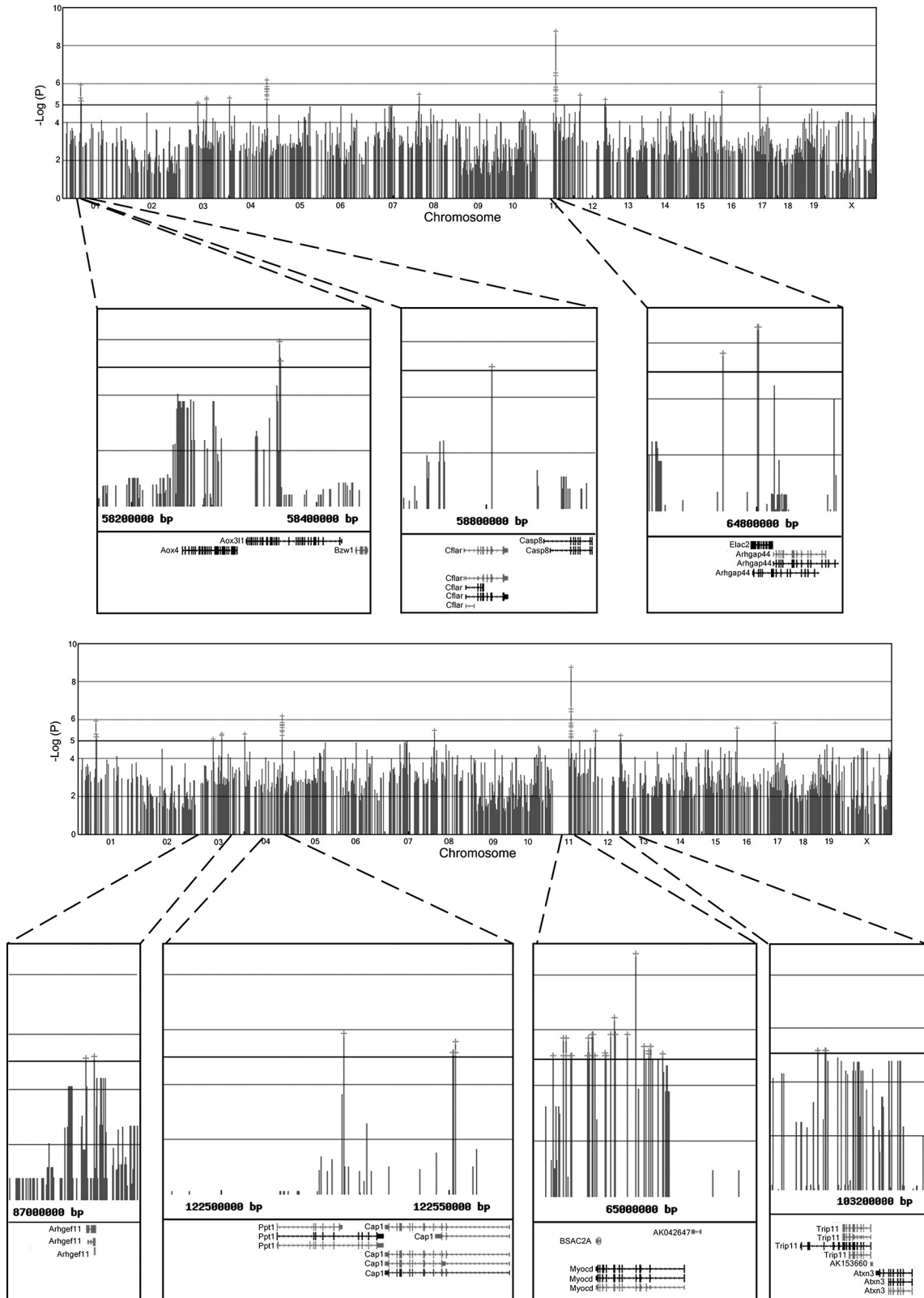


Fig. 5. Haplotype association mapping identifies susceptibility genes for cigarette smoke-independent bronchoalveolar lavage (BAL) double-stranded (ds) DNA levels. The Manhattan plot for the log-transformed BAL dsDNA levels depicts corresponding $-\log(P)$ association probabilities for single nucleotide polymorphisms (SNPs) at indicated chromosomal locations. The log-transformed BAL dsDNA levels of smoke- and air-exposed mice were used as input for the analysis, with air/smoke exposure added to the analysis as covariate. Significance level was set at SNP associations of $-\log(P) \leq 5$. Magnifications show genes mapped at the significant SNPs.

Table 4. Single nucleotide polymorphisms significantly associated with bronchoalveolar lavage double-stranded DNA levels after short-term cigarette smoke exposure in cigarette smoke-exposed mice

Chromosome No.	P Value	Position	Rsid	No. Major Alleles	No. Minor Alleles	No. Missing Alleles	Beta	Gene
3	5.44E-07	58655690	NES12922997	5	13	8	-0.193	<i>Clm1</i>
4	4.20E-06	122526998	NES09192855	14	9	3	0.153	<i>Ppt1</i>
4	3.05E-06	122551421	NES09192317	15	9	2	0.148	<i>Cap1</i>
4	7.94E-06	122612792	NES09190609	13	10	3	0.149	
4	1.05E-06	123538006	mm37-4-123538006	15	11	0	0.149	
4	5.64E-06	123571200	NES09195959	14	10	2	0.145	
4	7.94E-06	123635179	NES09194049	13	10	3	0.149	
4	7.94E-06	123636696	NES09194072	13	10	3	0.149	
4	7.94E-06	123670557	NES09193039	13	10	3	0.149	
4	7.94E-06	123671493	NES09192987	13	10	3	0.149	
4	7.94E-06	123671697	NES09192991	13	10	3	0.149	
4	7.94E-06	123671952	NES09192994	13	10	3	0.149	
4	7.94E-06	123672236	NES09192963	13	10	3	0.149	
4	7.94E-06	123672264	NES09192964	13	10	3	0.149	
7	5.50E-06	48487551	NES11797489	5	8	13	-0.176	
7	7.64E-06	48561882	NES11788344	5	9	12	-0.194	
7	7.64E-06	48564532	NES11788283	5	9	12	-0.194	
7	7.64E-06	48574462	NES11787752	5	9	12	-0.194	
7	5.10E-06	62427737	NES13966646	10	9	7	-0.146	<i>Luzp2</i>
7	5.10E-06	62428384	NES13966472	10	9	7	-0.146	<i>Luzp2</i>
7	5.10E-06	62428492	NES13966476	10	9	7	-0.146	<i>Luzp2</i>
7	5.10E-06	62429097	NES13966493	10	9	7	-0.146	<i>Luzp2</i>
7	5.10E-06	62429268	NES13966502	10	9	7	-0.146	<i>Luzp2</i>
7	6.64E-07	143830445	NES11531600	7	10	9	-0.142	
7	6.64E-07	143832205	NES11531519	7	10	9	-0.142	
7	6.64E-07	143834746	NES11531297	7	10	9	-0.142	
7	5.21E-06	145418830	NES11529417	6	9	11	-0.167	<i>Tcerg11</i>
8	7.81E-06	28527737	NES14961674	12	9	5	-0.155	
9	8.97E-09	45415420	NES15026605	10	12	4	-0.132	<i>Dscam11</i>
11	4.87E-09	64999358	NES08493493	9	13	4	-0.146	<i>Myocd</i>
11	1.73E-06	65014221	mm37-11-65014221	10	16	0	-0.137	<i>Myocd</i>
11	1.73E-06	65028777	mm37-11-65028777	10	16	0	-0.137	<i>Myocd</i>
11	3.03E-06	65014320	mm37-11-65014320	10	15	1	-0.138	<i>Myocd</i>
11	3.74E-06	65009295	NES08493388	10	15	1	-0.138	<i>Myocd</i>
11	3.74E-06	65016012	NES08493236	10	15	1	-0.138	<i>Myocd</i>
14	4.72E-07	77961027	NES12551493	7	12	7	-0.155	<i>Enox1</i>
14	2.04E-06	77952719	NES12551734	7	11	8	-0.156	<i>Enox1</i>
14	2.25E-06	78003520	mm37-14-78003520	7	19	0	-0.149	<i>Enox1</i>
14	4.88E-06	78017044	NES12548988	7	18	1	-0.149	<i>Enox1</i>
14	8.82E-06	78017551	NES12548996	7	17	2	-0.148	<i>Enox1</i>
14	8.82E-06	78017718	NES12548998	7	17	2	-0.148	<i>Enox1</i>
14	8.82E-06	78021491	NES12548821	7	17	2	-0.148	<i>Enox1</i>
14	8.82E-06	78025000	NES12548718	7	17	2	-0.148	<i>Enox1</i>
14	8.82E-06	78027930	NES12548591	7	17	2	-0.148	<i>Enox1</i>
14	8.82E-06	78031092	NES12548472	7	17	2	-0.148	<i>Enox1</i>
14	8.82E-06	78031958	NES12548481	7	17	2	-0.148	<i>Enox1</i>
16	4.25E-06	11870630	NES15692525	6	10	10	-0.160	<i>Cpped1</i>
17	6.86E-06	35534387	NES17324125	7	9	10	-0.158	<i>Bat1a</i>

Significance cutoff is set at $-\log(P) \geq 5$. Major and minor alleles indicate the number of mouse strains with the most and least abundant allele for the SNP, respectively. Missing alleles indicate the number of mouse strains with missing data for the SNP. SNP names and locations were based on mouse genome build 38.

CS-induced dysregulation of the expression of candidate genes in epithelium of humans susceptible for the onset of COPD. To investigate whether the candidate genes for CS-induced dsDNA release in mice are also regulated by CS exposure in the airway epithelium in human subjects, we analyzed the gene expression of our candidate genes in a microarray gene expression data set of primary bronchial epithelial cells obtained from bronchial brushings of young, healthy individuals. These cells were isolated 24 h after smoking of three cigarettes within 3 h and after 2 days of smoking cessation, as described previously (54). Out of the 11 candidate genes, we analyzed expression regulation of 10 candidate genes, since the mouse *Aox311* gene does not have

a human homolog. We found that the gene expression levels of *ARHGAP44* and *ENOX1* were significantly decreased by exposure to CS (Table 7). None of the eight other candidate genes showed significant changes in gene expression on CS exposure. The young, healthy individuals included in this study were selected to be either susceptible or nonsusceptible for the development of COPD based on family history, as described before (24, 54). In brief, the prevalence of COPD in smoking first- or second-degree relatives older than 40 yr was used to classify the young, healthy subjects as susceptible (at least 2 out of 3 first- and second-degree smoking relatives developed COPD) or nonsusceptible (none of the smoking first- and second-degree relatives

Table 5. Selected single nucleotide polymorphisms significantly associated with bronchoalveolar lavage double-stranded DNA levels after short-term cigarette smoke exposure in cigarette smoke-exposed mice

Chromosome No.	P Value	Position	Rsid	No. Major Alleles	No. Minor Alleles	No. Missing Alleles	Beta	Variation Type/ Function Class	BALB/ cByJ	PL/J	C58/J	A/J	Gene
4	4.20E-06	122526998	NES09192855	14	9	3	0.153	Int	A	A	uk	C	<i>Ppt1</i>
4	3.05E-06	122551421	NES09192317	15	9	2	0.148	Int	G	G	G	A	<i>Cap1</i>
9	8.97E-06	45415420	NES15026605	10	12	4	-0.132	Int	T	C	T	T	<i>Dscam1l</i>
11	4.87E-09	64999358	NES08493493	9	13	4	-0.146	Int	T	T	C	C	<i>Myocd</i>
11	1.73E-06	65014221	mm37-11-65014221	10	16	0	-0.137	Int	C	C	T	T	<i>Myocd</i>
11	1.73E-06	65028777	mm37-11-65028777	10	16	0	-0.137	Int	A	A	G	G	<i>Myocd</i>
11	3.03E-06	65014320	mm37-11-65014320	10	15	1	-0.138	CsP:227	G	G	C	C	<i>Myocd</i>
11	3.74E-06	65009295	NES08493388	10	15	1	-0.138	Int	C	C	T	T	<i>Myocd</i>
11	3.74E-06	65016012	NES08493236	10	15	1	-0.138	Int	G	G	A	A	<i>Myocd</i>
14	2.25E-06	78003520	mm37-14-78003520	7	19	0	-0.149	Int	A	G	A	A	<i>Enox1</i>
14	4.88E-06	78017044	NES12548988	7	18	1	-0.149	Int	G	A	G	G	<i>Enox1</i>
14	8.82E-06	78017551	NES12548996	7	17	2	-0.148	Int	G	A	G	G	<i>Enox1</i>
14	8.82E-06	78017718	NES12548998	7	17	2	-0.148	Int	C	T	C	C	<i>Enox1</i>
14	8.82E-06	78021491	NES12548821	7	17	2	-0.148	Int	C	T	C	C	<i>Enox1</i>
14	8.82E-06	78025000	NES12548718	7	17	2	-0.148	Int	G	T	G	G	<i>Enox1</i>
14	8.82E-06	78027930	NES12548591	7	17	2	-0.148	Int	C	A	C	C	<i>Enox1</i>
14	8.82E-06	78031092	NES12548472	7	17	2	-0.148	Int	A	T	A	A	<i>Enox1</i>
14	8.82E-06	78031958	NES12548481	7	17	2	-0.148	Int	C	T	C	C	<i>Enox1</i>

Significant SNPs were located within a gene and had less than six mouse strains with missing data. Significance cutoff is set at $-\log(P) \geq 5$. Number of major and minor alleles indicates the number of mouse strains with the most and least abundant allele for the SNP, respectively, from the 28 mouse strains used in our analyses. Number of missing alleles indicates the number of mouse strains with missing data for the SNP. Function class is intronic (Int), synonymous-codon (Cs) with the amino acid and location. Position is the base pair location of the SNP. SNP names and locations were based on mouse genome build 38.

developed COPD). When analyzing the interaction between CS exposure and susceptibility for COPD as defined by family history, we observed that the mRNA expression levels of *ARHGEF11* and *ENOX1* were significantly more decreased by CS in COPD-susceptible individuals compared with nonsusceptible individuals. Interestingly, in mice, the mRNA expression levels of these transcripts were decreased by CS in the nonsusceptible strains. In addition, the *ELAC2* gene showed a trend ($P = 0.085$) toward a CS-induced decrease between susceptible and nonsusceptible individuals. These data indicate that specific identified susceptibility genes for CS-induced dsDNA release in mice are also differently expressed by CS in relation to susceptibility for the development of COPD in humans.

Downregulation of candidate genes in human alveolar epithelial cells influences CS-induced cell death and DAMP release. Since *Ppt1* and *Elac2* showed an interaction between the effect of their expression regulation and susceptibility for CS-induced dsDNA release, we selected these two genes for further investigation. Furthermore, since the expression of *ENOX1*, *ARHGEF11*, and *ARHGAP44* was affected by CS exposure in human bronchial epithelial cells we also selected these genes for further investigation. We studied the effect of downregulation of these candidate genes in human lung epithelial cells on CSE-induced cell death and DAMP release.

First, we tested which of three human lung epithelial cell lines was most suitable for CSE-induced dsDNA release experiments. Therefore, the bronchial epithelial cell lines 16HBE and BEAS-2B and the adenocarcinoma alveolar cell line A549 were exposed to 0–100% of CSE for 4 h. After extensive washing and incubation for another 16 h on CSE-free medium, the amount of dsDNA in the cell-free supernatant was determined. Neither BEAS-2B nor 16HBE cells showed a significant increase in the amount of dsDNA release on CSE exposure, whereas A549 cells showed a dose-dependent increase in the amount of dsDNA that is released on CSE exposure (Fig.

9A). Therefore, further experiments to test the effects of the selected candidate genes on CS-induced dsDNA release were performed using A549 cells.

Transfection of the human airway epithelial cell line A549 with specific siRNA for *PPT1* induced >95% mRNA downregulation (Fig. 9B). After the siRNA transfection, cells were exposed to a range of CSE concentrations (0–100%) for 4 h. After 24 h of incubation with CSE-free medium, the amount of necrotic and apoptotic cells and dsDNA release was determined. On stimulation with high percentages of CSE (80–100%), *PPT1* downregulation resulted in increased release of dsDNA and RNA and increased levels of both apoptotic and necrotic cell death (Fig. 9). This indicates that *PPT1* downregulation enhances the susceptibility of A549 cells to cell death and DAMP release induced by high-CSE concentrations.

Downregulation of *ELAC2* using specific siRNA assays induces ~80% decrease in mRNA expression (Fig. 10A). Downregulation of *ELAC2* significantly attenuated dsDNA release on exposure to 60% CSE, apoptotic cell death on exposure to 0–80% CSE, and necrotic cell death on exposure to 0–40% CSE compared with the scrambled control (Fig. 10).

ARHGAP44 was not expressed in A549 cells, disqualifying this gene as target for siRNA experiments in A549 cells (data not shown). Downregulation of *ENOX1* resulted in >90% decreased mRNA expression levels (Fig. 11A). Although no effects of *ENOX1* downregulation on DAMP release or necrotic cell death induced by CS exposure was observed, we did find that *ENOX1* downregulation decreased the percentage of apoptotic cells at baseline conditions (Fig. 11, B–F). Moreover, downregulation of *ARHGEF11* using specific siRNA assays decreased the mRNA expression with >80% (Fig. 11G). No effects of *ARHGEF11* downregulation on DAMP CS-induced release were found. Nevertheless, we did observe that, on CS exposure, significantly more cells are necrotic on downregulation of *ARHGEF11* (Fig. 11, H–L). This suggests that decreased *ARHGEF11* expression increases the susceptibility for

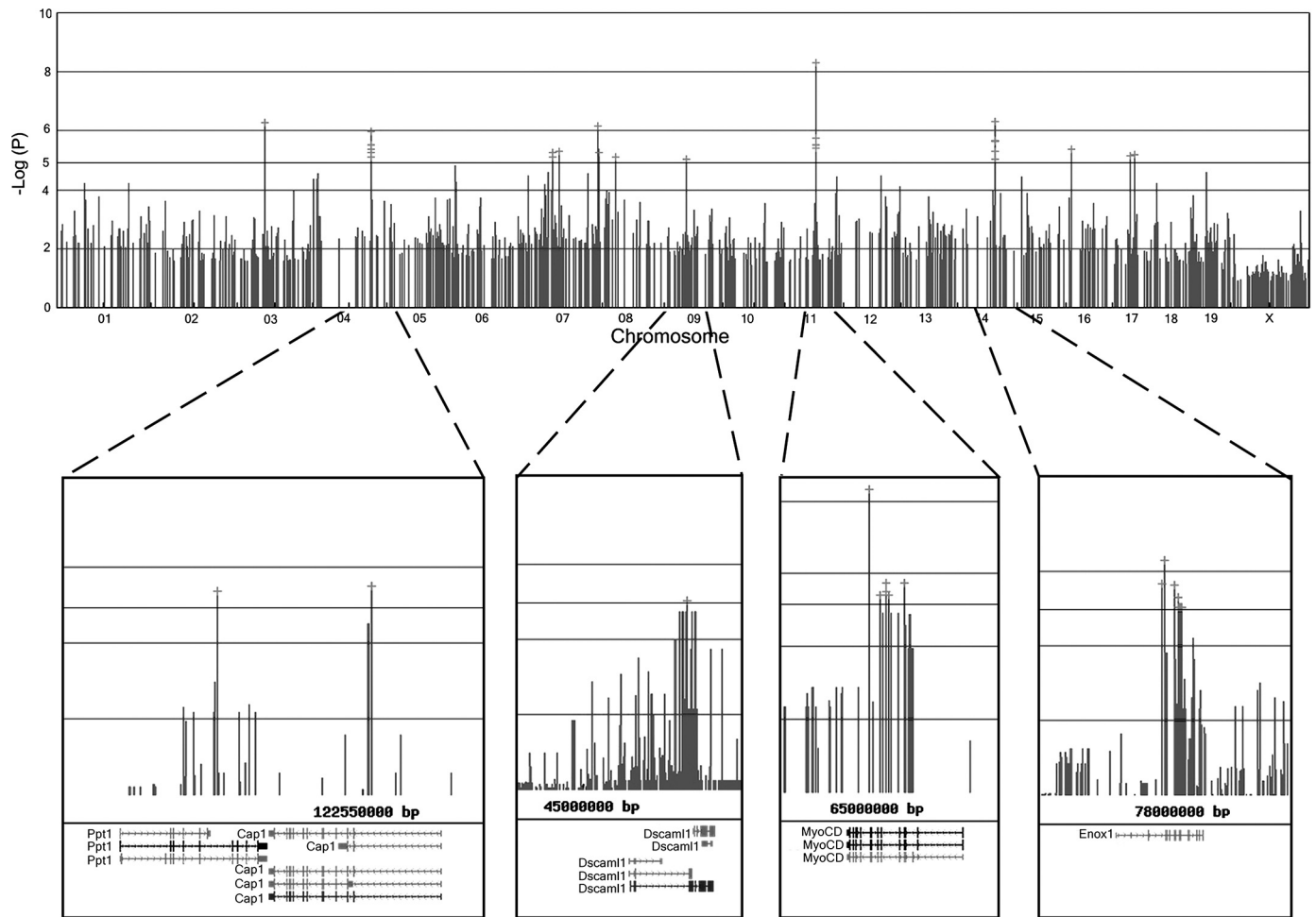


Fig. 6. Haplotype association mapping identifies susceptibility genes for cigarette smoke-induced bronchoalveolar lavage (BAL) double-stranded (ds) DNA levels. The Manhattan plot for the log-transformed cigarette smoke-induced BAL dsDNA levels depicts corresponding $-\log(P)$ association probabilities for single nucleotide polymorphisms (SNPs) at indicated chromosomal locations. The log-transformed BAL dsDNA levels of only smoke-exposed mice were used as input for the analysis. BALB/cJ and BALB/cByJ mice were excluded from this analysis. Significance level was set at SNP associations of $-\log(P) \leq 5$. Magnifications show genes mapped at the significant SNPs.

CS-induced necrotic cell death, which is in agreement with our gene expression data in human bronchial epithelial cells (Table 7), showing that *ARHGEF11* expression is more decreased on CS exposure in individuals susceptible for COPD compared with nonsusceptible individuals.

In summary, downregulation of *ELAC2* provides protection against CSE-induced cell death and DAMP release on exposure to low percentages of CSE, whereas downregulation of *PPT1* and *ARHGEF11* enhances CSE-induced cell death and DAMP release on exposure to high percentages of CSE.

DISCUSSION

In the present study, we show that CS-induced DAMP release differs between inbred mouse strains and is genetically regulated by specific genes. We identified 11 candidate genes involved in BAL dsDNA levels in mice, 5 of which were associated with CS-induced dsDNA release. For two of these candidate genes, *Ppt1* and *Elac2*, we observed that these SNPs act as an eQTL in lung tissue and display an interaction with susceptibility for CS-induced dsDNA release, indicating that these genes may contribute to the differences in dsDNA release

between susceptible and nonsusceptible strains. We found that these genes are functionally involved in CS-induced cell death and DAMP release in a human lung epithelial cell line. In addition, we show that two other candidate genes, *ARHGEF11* and *ENOX1*, decreased more in young susceptible individuals compared with nonsusceptible individuals. In addition, *ELAC2* trended toward a decrease. Taken together, these data indicate that the severity of CS-induced airway inflammation might be caused by differences in the sensitivity for CS-induced DAMP release.

The role of DAMPs in the pathophysiology of COPD is emerging (47). DAMPs are released from necrotic or damaged cells and activate the innate immune system by activation of PRRs and by attracting neutrophils (44). Previously, our laboratory has shown that exposure of human airway epithelial cells to CSE induces DAMP release and subsequent proinflammatory responses (23, 50). Furthermore, our laboratory has shown that exposure of mice to CS induces the release of a specific profile of DAMPs in mice susceptible for CS-induced neutrophilic airway inflammation compared with those strains that are not susceptible to this response (48). In the present

Table 6. Genes with significant single nucleotide polymorphism associations with bronchoalveolar lavage double-stranded DNA levels after short-term cigarette smoke exposure in mice

Symbol	Description	Gene ID	Chromosome No.	Protein Function
<i>Aox3l1</i>	Aldehyde oxidase 2	213043	1	Molybdo-flavoenzyme family member that oxidizes aldehydes and is involved in the perception of odorants (32).
<i>Cflar</i>	CASP8 (caspase 8) and FADD (Fas-associated protein with death domain)-like apoptosis regulator	12633	1	Apoptosis and necroptosis regulator protein (22).
<i>Arhgef11</i>	Rho guanine nucleotide exchange factor (GEF) 11	2441869	3	Rho-GTPase, involved in rho-dependent signaling (26).
<i>Ppt1</i>	Palmitoyl-protein thioesterase 1	19063	4	Lipid modification during lysosomal degradation, removal of thioester-linked fatty acyl groups from cysteine residues. Regulation of TNF- α -induced apoptosis (55).
<i>Cap1</i>	Adenylate cyclase-associated protein 1	88262	4	Actin-binding cyclic AMP signaling molecule and potent inducer of apoptosis (3).
<i>Dscaml1</i>	Down syndrome cell adhesion molecule like 1	2150309	9	Member of the immunoglobulin superfamily proteins (17).
<i>Elac2</i>	ElaC homolog 2	68626	11	Catalyzing the removal of the 3' trailer from precursor tRNAs. The DNA damage response (52).
<i>Arhgap44</i>	Rho GTPase activating protein 44	2144423	11	Rho-GTPase, involved in rho-dependent signaling (18).
<i>Myocd</i>	Myocardin	214384	11	A smooth muscle and cardiac muscle-specific transcriptional coactivator of the transcription factor SRF (41).
<i>Trip11</i>	Thyroid hormone receptor interactor 11	1924393	12	Thyroid hormone receptor- β interaction and association with microtubules and the Golgi-apparatus (15).
<i>Enox1</i>	Ecto-NOX disulfide-thiol exchanger 1	2444896	14	Electron transport protein, terminal oxidase of plasma electron transport from cytosolic NAD(P)H via hydroquinones to acceptors at the cell surface. Inhibitor of apoptosis (57).

study, we employed our existing data set of 28 different inbred mouse strains exposed to CS for 5 consecutive days (46). We found increased levels of all measured DAMPs, i.e., HSP70, HMGB1, mtDNA, and dsDNA, in BAL fluid of several but not all mouse strains. The levels of dsDNA showed the highest correlation with CS-induced neutrophil infiltration in BAL fluid, in agreement with our laboratory's previous study (48). dsDNA is a widely abundant DAMP that is released by necrotic cells and is not likely to be actively secreted, with the exception of neutrophils undergoing NETosis, making dsDNA a good marker for necrotic cell death (38, 49). Other DAMPs, including HSP70 and HMGB1, can both be passively released and actively secreted from several cell types upon stress (5). It is possible that part of the dsDNA levels found in BAL fluid is derived from cell lysis during BAL extraction; nevertheless the fact that we found large amounts of nonlysed cells on analyzing cytopins and the lack of correlation between the different DAMPs renders it unlikely that much cell lysis has taken place during BAL extraction. Furthermore, it is likely that the strong correlation between the CS-induced levels of dsDNA in BAL fluid and the number of neutrophils in BAL fluid can at least, in part, be explained by neutrophils being the source of the released dsDNA. Nevertheless, the first line of defense against inhaled toxicants is the airway epithelium, providing the first batch of DAMP release, followed by DAMP released from attracted neutrophils (47). Furthermore, it has been shown that the sputum levels of dsDNA are negatively correlated with percent predicted forced expiratory volume in 1 s in patients with cystic fibrosis (39), indicating that dsDNA release is involved in multiple diseases associated with decreased lung function.

In the present study, we identified 11 genes that are significantly associated with dsDNA release in mice. First we

analyzed which genes were associated with basal dsDNA release, which identified nine genes. Next, we identified two additional genes that were specifically associated with CS-induced dsDNA release. In the second analysis investigating CS-induced dsDNA release, we removed the BALB/cByJ and BALB/cJ strains because the high induction of CS-induced dsDNA release in these strains was masking the identification of susceptibility genes. Nevertheless, this approach may introduce false-negative results, as the two most susceptible strains were not included in the analysis. This may also explain the lack of overlap in identified susceptibility genes between the present study and our laboratory's previous work where we analyzed genetic susceptibility for CS-induced neutrophilic airway inflammation in mice (46). Two of the identified susceptibility genes, *Dscaml1* and *Enox1*, were specifically associated with CS-induced dsDNA release. No direct link in function was observed for these 11 genes using gene ontology annotation. However, five genes have known involvement in cell death pathways, as *Cflar*, *Ppt1*, *Cap1*, *Enox1*, and *Elac2* have been shown to be involved in apoptosis and DNA damage responses, indicating that a dysfunctional induction of apoptosis induces increased levels of released dsDNA. *Cflar*, also called c-Flip, is one of the major components in the apoptotic pathways, and it regulates whether a cell goes into apoptosis or necroptosis (53), making *Cflar* a relevant candidate gene as apoptotic cells do not release dsDNA, while necroptotic cells do. Moreover, it has been shown that *Cflar* protects murine fibroblasts against dsRNA-induced apoptosis (21). *Ppt1* is involved in the regulation of apoptosis: on one hand *Ppt1* overexpression induces protection against the induction of apoptosis (9, 13), and inhibition of *Ppt1* induces apoptosis in neuronal cells (10, 11, 20). While on the other hand PPT1-deficient fibroblasts from mice and humans were protected

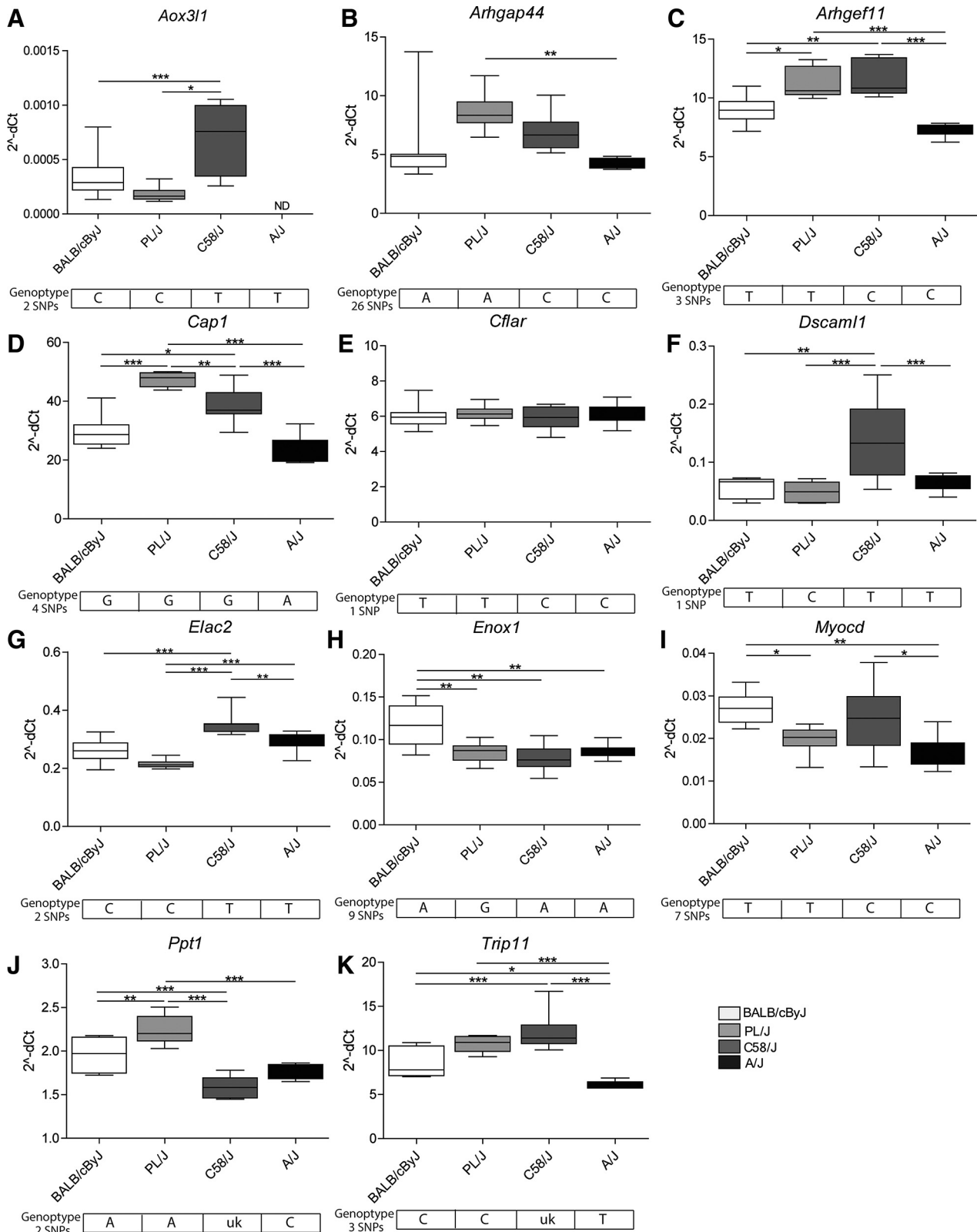


Fig. 7. Gene expression of candidate genes in whole lung tissue of susceptible and nonsusceptible mouse strains. Four mouse strains were selected (BALB/cByJ, PL/J, C58/J, A/J) with a different susceptibility for cigarette smoke-induced double-stranded (ds) DNA release in bronchoalveolar lavage (BAL) fluid, ranging from the highly susceptible BALB/cByJ to the resistant A/J strain. Basal mRNA expression ($2^{-\Delta\Delta C_t}$) was measured in air-exposed mice for *Aox311* (A), *Arhgap44* (B), *Arhgef11* (C), *Cap1* (D), *Cflar* (E), *Dscaml1* (F), *Elac2* (G), *Enox1* (H), *Myocd* (I), *Ppt1* (J), and *Trip11* (K). Genotypes are shown for each gene; a representative genotype was selected for genes associated with a haplotype of multiple single nucleotide polymorphisms (SNPs). Data are shown as box-whisker plots, indicating the mean \pm interquartile range, with the whiskers indicating the highest and lowest data points. Significance was tested using a one-way ANOVA with Turkey's multiple-comparison correction. * $P < 0.05$, ** $P \leq 0.01$, and *** $P \leq 0.001$.

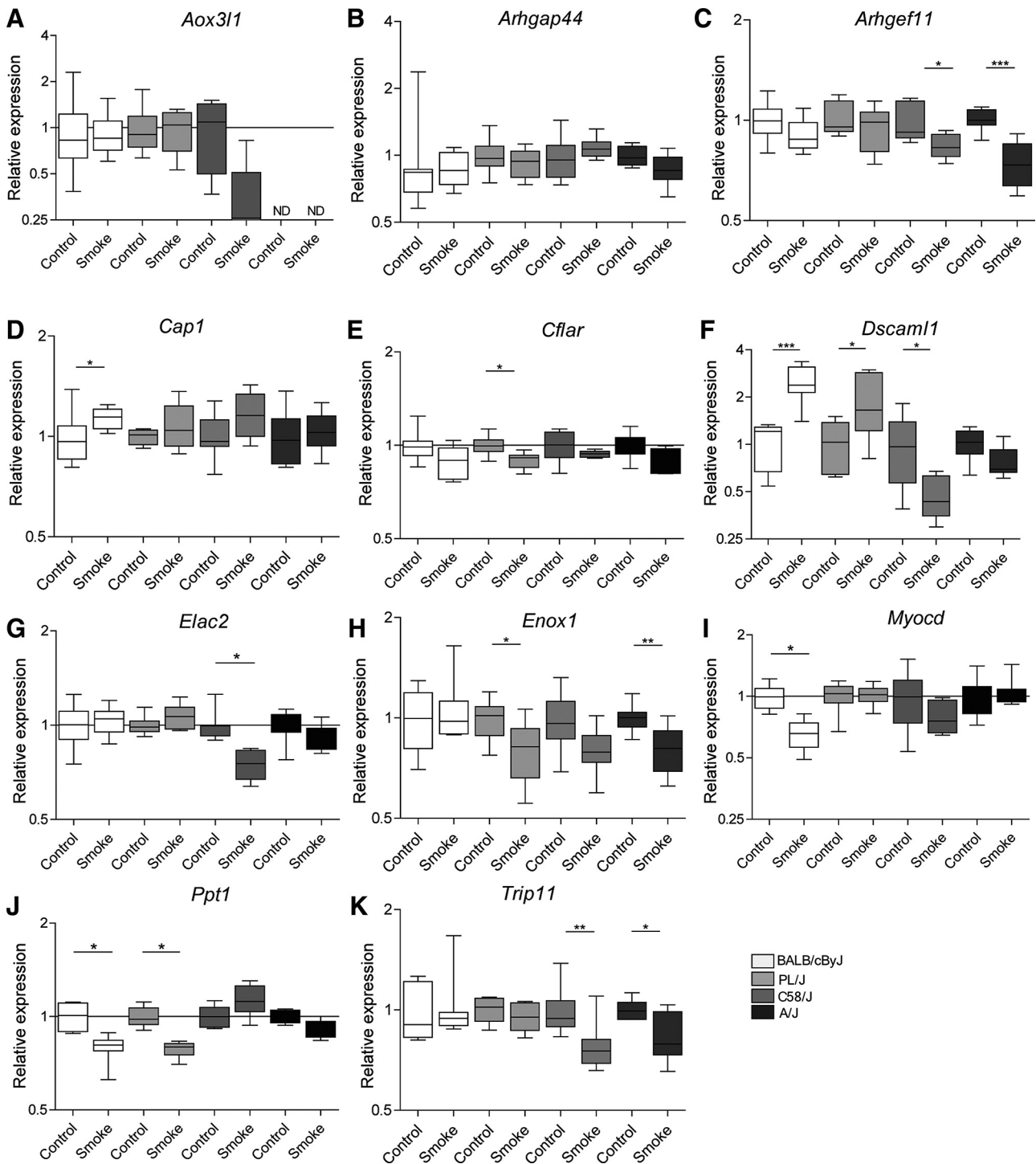


Fig. 8. Cigarette smoke-induced gene expression of candidate genes in whole lung tissue of susceptible and nonsusceptible mouse strains. Four mouse strains were selected (BALB/cByJ, PL/J, C58/J, A/J) with a different susceptibility for cigarette smoke-induced double-stranded (ds) DNA release in bronchoalveolar lavage (BAL) fluid, ranging from the highly susceptible BALB/cByJ to the resistant A/J strain. mRNA expression was shown as fold induction of 2^{-ΔCt} of cigarette smoke-exposed mice ($n = 8$) compared with 2^{-ΔCt} of control air-exposed mice ($n = 8$) for *Aox311* (A), *Arhgap44* (B), *Arhgef11* (C), *Cap1* (D), *Cflar* (E), *Dscaml1* (F), *Elac2* (G), *Enox1* (H), *Myocd* (I), *Ppt1* (J), and *Trip11* (K). Data are shown as box-and-whisker plots, indicating the mean \pm interquartile range, with the whiskers indicating the highest and lowest data points. Significance was tested using a Mann-Whitney *U*-test. * $P < 0.05$, ** $P \leq 0.01$, and *** $P \leq 0.001$.

against TNF-induced apoptosis, and restoration of PPT1 increased the susceptibility for apoptosis (55). This indicates that the effect of Ppt1 on cell death is cell type specific. Cap1 is also involved in apoptosis, as the induction of apoptosis induces the caspase-independent translocation of Cap1 to the mitochondria,

which is important for the execution of apoptosis, while the downregulation of *Cap1* represses the execution of apoptosis (58). Furthermore, for *Enox1*, chemical or genetic inhibition induces apoptosis (19). *Elac2* was shown to be involved in the DNA damage response (52), which also links it to dsDNA

Table 7. Gene expression of candidate genes in humans susceptible or nonsusceptible for the onset of chronic obstructive pulmonary disease

	Smoke Exposure			Smoke Exposure Interaction with Susceptibility		
	<i>t</i> value	<i>P</i> value	FDR	<i>t</i> value	<i>P</i> value	FDR
<i>ARHGAP44</i>	-2.526	0.017	0.168	-0.925	0.362	0.604
<i>ARHGEF11</i>	-1.152	0.258	0.430	-2.060	0.048	0.241
<i>CAP1</i>	0.806	0.426	0.609	0.433	0.668	0.835
<i>CFLAR</i>	-0.513	0.612	0.679	0.116	0.909	0.909
<i>DSCAML1</i>	-1.443	0.159	0.397	-1.082	0.288	0.576
<i>ELAC2</i>	-0.682	0.500	0.625	-1.779	0.085	0.285
<i>ENOX1</i>	-2.224	0.034	0.168	-2.062	0.048	0.241
<i>MYOCD</i>	1.238	0.225	0.430	-0.310	0.758	0.843
<i>PPT1</i>	1.742	0.092	0.305	0.568	0.574	0.821
<i>TRIP11</i>	0.221	0.826	0.826	1.393	0.174	0.435

Microarray results for smoke exposure show the effects of smoking three cigarettes within 3 h on gene expression levels in young (age \leq 40 yr) individuals either susceptible or nonsusceptible for the onset of COPD. Smoke exposure interaction with susceptibility indicates significance in gene expression for the delta before and after smoking three cigarettes between susceptible and nonsusceptible individuals. False discovery rate (FDR) \leq 0.25 for significance.

release. For the remaining six genes, no connection to cell death or dsDNA release is known to date; however, much is unknown about the function of these genes. Of the six genes, for *Arhgef11*, *Dscaml1*, and *Trip11*, as well as for *Ppt1* and *Elac2*, a correlation was shown between the CS-induced gene expression in whole lung tissue of mice and the susceptibility for CS-induced DAMP release. Of note, only for *Elac2* and *Ppt1* were the observed differences in CS-induced gene expression between susceptible and nonsusceptible mouse strains in agreement with the genotype of the SNPs associated with the dsDNA levels in the genetic analysis, underscoring that these SNPs possibly act as an eQTL for these genes. For *Ppt1*, the gene expression was significantly lower in nonsusceptible mouse strains compared with susceptible mouse strains, whereas exposure to CS decreases the *Ppt1* expression in the susceptible mouse strains. For *Elac2*, the situation was opposite, with increased expression in nonsusceptible mouse strains compared with susceptible mouse strains and a downregulation in gene expression by CS exposure in the nonsusceptible strains. The interaction of gene regulation of these two candidate genes with susceptibility for CS-induced dsDNA release strongly argues in favor for a contribution of these genes to the susceptibility for CS-induced dsDNA release.

For the two key candidate genes, *Ppt1* and *Elac2*, we showed that downregulation induces protection against CSE-induced cell death and DAMP release on exposure to low percentages of CSE, while it enhances CSE-induced cell death and DAMP release on exposure to high percentages of CSE in vitro in alveolar epithelial cells. The results at low CSE percentages are in agreement with a previous study showing that inhibition of *PPT1* decreases the amount of apoptosis in absence of CSE (55). Furthermore, we showed that the CS-induced decrease in *ARHGEF11* expression was greater in young, healthy individuals susceptible for the development of COPD compared with nonsusceptible individuals. This is in agreement with our in vitro data showing that downregulation of *ARHGEF11* in A549 cells causes more cells to go into necrosis on CS exposure. These results show that our candidate

genes are not solely important in CS-induced dsDNA release in mice, but are also functionally involved in CS-induced cell death and DAMP release in human cells in vitro, making them interesting targets for future research.

The relevance of our candidate genes for COPD patients was further supported by the fact that we identified two genes, *ARHGAP44* and *ENOX1*, of which the expression was decreased in human bronchial epithelial cells 24 h after smoking three cigarettes in young, healthy individuals. Importantly, the gene expression of *ARHGEF11* and *ENOX1* was significantly more decreased by smoking three cigarettes in young, healthy individuals who are susceptible for the development of COPD compared with young, healthy individuals who are not. Furthermore, *ELAC2* showed a trend toward a stronger CS-induced decrease in susceptible compared with nonsusceptible individuals. Although there was a discrepancy between the effect of CS on the expression of *ARHGEF11* and *ENOX1* in susceptible vs. nonsusceptible humans and mouse strains, with a stronger decrease by CS exposure in susceptible humans and in nonsusceptible mouse strains, our results show that, before the onset of COPD, these genes are already dysregulated, making them likely candidate genes to be causally involved in the disease pathophysiology. Differences in gene expression between our mice and human studies are likely to be caused by differences in the levels of CS exposure, timing, and the composition of the investigated cells. Further research is needed to fully elucidate the role of these genes in COPD pathophysiology. Although effectiveness of the classification of susceptible and nonsusceptible human individuals in the COPD susceptibility cohort was shown before (16, 24), the study setup is prone to induce false positive and negative classifications. First, the (non)susceptibility traits that are present in smoking first- or second-degree relatives diagnosed with or without COPD are not necessarily inherited by the next generation, potentially leading to false positive or negative classifications. Second, genetic recombination and de novo mutations can lead to the presence of susceptibility traits that are not present in nonsusceptible relatives, potentially inducing false negative classifications. Together, the statistical power of the study is limited by the probable number of false positive and negative classifications; nevertheless, we were still able to show significant differences between susceptible and nonsusceptible individuals.

In summary, with the present study, we have identified 11 novel candidate genes for CS-induced dsDNA release in mice. With several validation experiments in both mice and humans, we have shown functional or expression-based involvement of eight of the genes in CS-induced cell death and DAMP release. Two key candidate genes were shown to be involved in CSE-induced cell death and DAMP release in the human airway epithelium. These genes are possibly involved in the pathogenesis of diseases, where CS exposure induces dsDNA release and subsequent inflammation, e.g., COPD (47, 48). Further research is needed to elucidate the functional role of the candidate genes in dsDNA release in general and in COPD in specific.

GRANTS

This study was funded by The Lung Foundation Netherlands (<https://www.longfonds.nl>) (project 6.2.15.044JO received by S. D. Pouwels, and project 3.2.11.025 received by M. C. Nawijn) and Top Institute Pharma

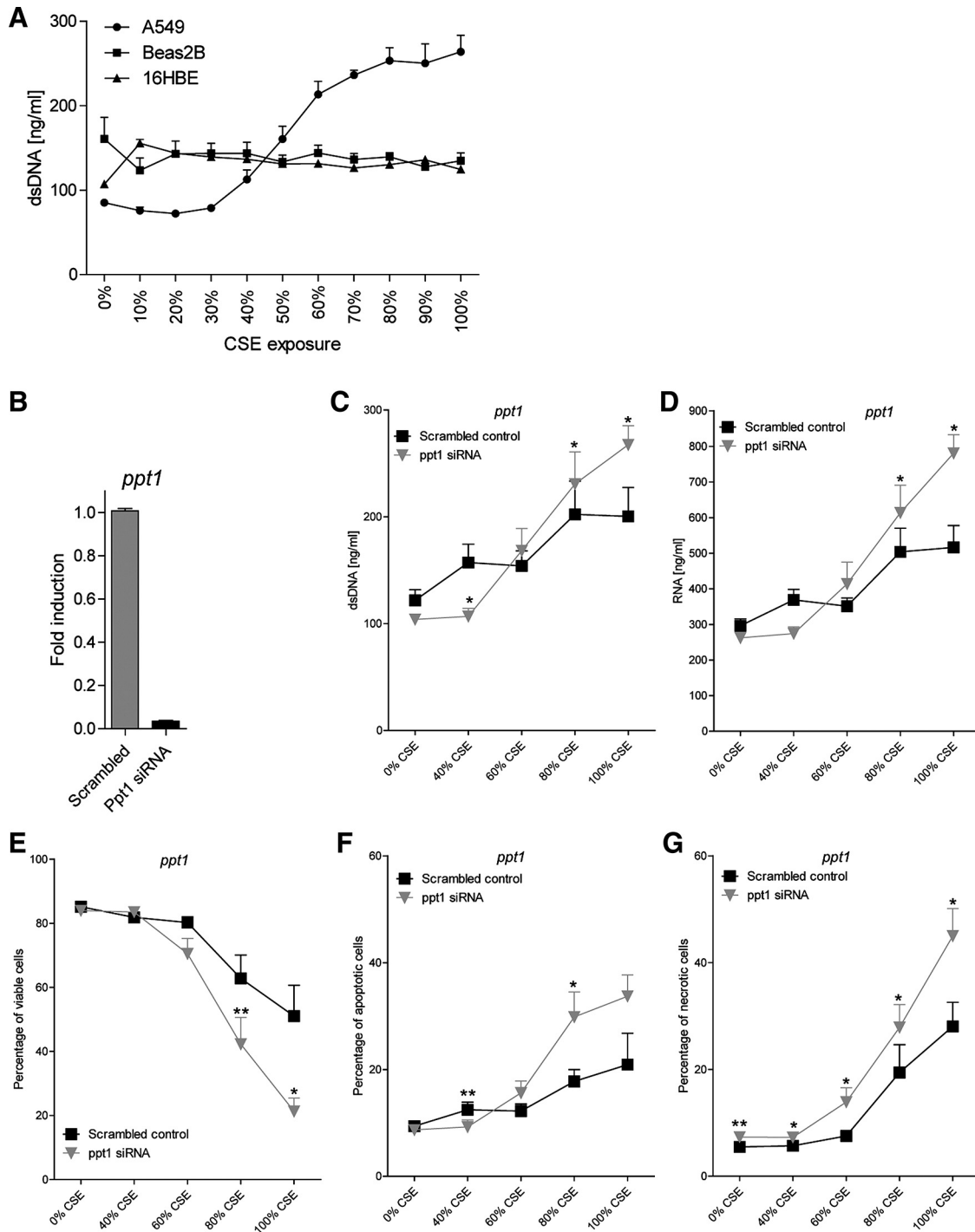


Fig. 9. The effect of downregulation of *PPT1* on damage-associated molecular pattern (DAMP) release and cell death in human alveolar epithelial cells. A: the human bronchial epithelial cell lines BEAS-2B and 16HBE and the alveolar adenocarcinomic cell line A549 were exposed to a range of cigarette smoke extract (CSE) for 4 h (0–100%). The levels of double-stranded (ds) DNA were measured in supernatant after 16 h of incubation with serum-free and CSE-free medium. B: the level of downregulation of *PPT1* in A549 cells on treatment with specific small interfering (si) RNA, as analyzed with quantitative RT-PCR, is shown. Data are shown as fold induction of mRNA expression of A549 cells treated with scrambled siRNA assay ($2^{-\Delta\Delta Ct}$) compared with A549 cells treated with siRNA assay specific for *PPT1* ($2^{-\Delta\Delta Ct}$). The levels of dsDNA (C) and RNA (D) were measured in cell-free supernatant of A549 cells exposed to 0–100% CSE. Scrambled control represents cells treated with scrambled siRNA assay, and *PPT1* siRNA is treated with specific siRNA assays. The levels of viable (E), apoptotic (F), and necrotic cells (G) were analyzed in A549 cells on exposure to 0–100% CSE using annexin/propidium iodide staining for flow cytometry. All data are shown as means \pm SE of the mean. Significance was tested using a Mann-Whitney *U*-test. * $P < 0.05$ and ** $P \leq 0.01$.

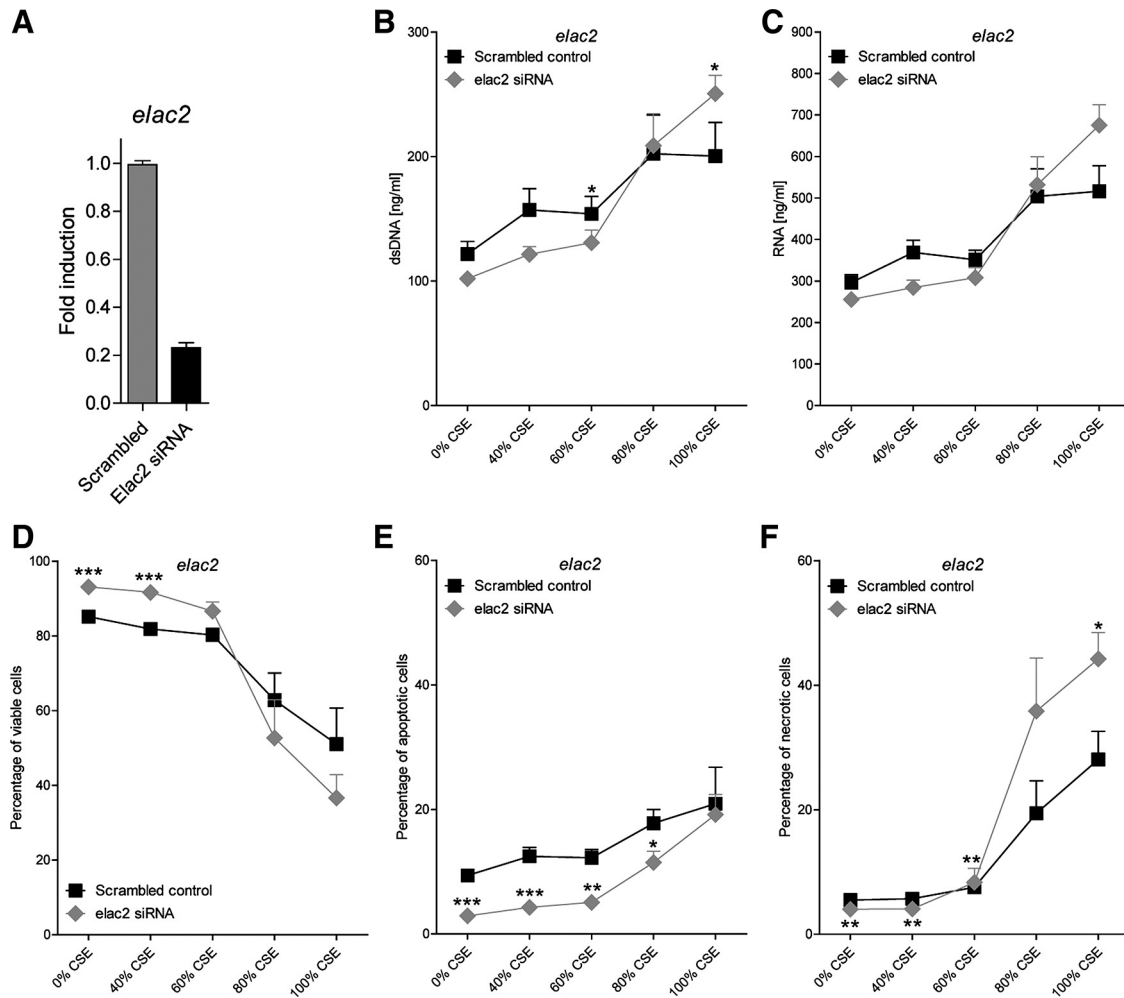


Fig. 10. The effect of downregulation of *ELAC2* on damage-associated molecular pattern (DAMP) release and cell death in human alveolar epithelial cells. A: the level of downregulation of *ELAC2* in A549 cells on treatment with specific small interfering (si) RNA analyzed, as by quantitative RT-PCR, is shown. Data are shown as fold induction of mRNA expression of A549 cells treated with scrambled siRNA assay ($2^{-\Delta\Delta C_t}$) compared with A549 cells treated with siRNA assay specific for *ELAC2* ($2^{-\Delta\Delta C_t}$). The levels of double-stranded (ds) DNA (B) and RNA (C) were measured in cell-free supernatant of A549 cells exposed to 0–100% CSE. Scrambled control represents cells treated with scrambled siRNA assay, and *ELAC2* siRNA is treated with specific siRNA assays. The levels of viable (D), apoptotic (E), and necrotic (F) cells were analyzed in A549 cells on exposure to 0–100% CSE using annexin/propidium iodide staining for flow cytometry. Values are means \pm SE of the mean. Significance was tested using a Mann-Whitney U-test. * $P < 0.05$, ** $P \leq 0.01$, and *** $P \leq 0.001$.

(<http://www.tipharma.com/home>) (project T1–201 received by N. T. H. ten Hacken).

DISCLOSURES

No conflicts of interest, financial or otherwise, are declared by the authors.

AUTHOR CONTRIBUTIONS

S.D.P., R.K., N.H.t.H., A.J.v.O., M.v.d.B., I.H.H., M.C.N. conceived and designed research; S.D.P., A.F., L.E.d.B., and R.G. performed experiments; S.D.P., A.F., M.v.d.B., H.M.B., and M.C.N. analyzed data; S.D.P., A.F., H.M.B., R.K., N.H.t.H., A.J.v.O., I.H.H., and M.C.N. interpreted results of experiments; S.D.P. and A.F. prepared figures; S.D.P. and M.C.N. drafted manuscript; S.D.P., A.F., M.v.d.B., H.M.B., R.K., N.H.t.H., A.J.v.O., I.H.H., and M.C.N. edited and revised manuscript; S.D.P., A.F., L.E.d.B., R.G., M.v.d.B., H.M.B., R.K., N.H.t.H., A.J.v.O., I.H.H., and M.C.N. approved final version of manuscript.

REFERENCES

- Andersen CL, Jensen JL, Ørntoft TF. Normalization of real-time quantitative reverse transcription-PCR data: a model-based variance estimation approach to identify genes suited for normalization, applied to

- bladder and colon cancer data sets. *Cancer Res* 64: 5245–5250, 2004. doi:10.1158/0008-5472.CAN-04-0496.
- Antunes MA, Abreu SC, Silva AL, Parra-Cuentas ER, Ab’Saber AM, Capelozzi VL, Ferreira TPT, Martins MA, Silva PMR, Rocco PR. Sex-specific lung remodeling and inflammation changes in experimental allergic asthma. *J Appl Physiol* (1985) 109: 855–863, 2010. doi:10.1152/jappphysiol.00333.2010.
- Bahn YS, Sundstrom P. CAP1, an adenylate cyclase-associated protein gene, regulates bud-hypha transitions, filamentous growth, and cyclic AMP levels and is required for virulence of *Candida albicans*. *J Bacteriol* 183: 3211–3223, 2001. doi:10.1128/JB.183.10.3211-3223.2001.
- Bennett BJ, Farber CR, Orozco L, Kang HM, Ghazalpour A, Siemers N, Neubauer M, Neuhaus I, Yordanova R, Guan B, Truong A, Yang WP, He A, Kayne P, Gargalovic P, Kirchgessner T, Pan C, Castellani LW, Kostem E, Furlotte N, Drake TA, Eskin E, Lusis AJ. A high-resolution association mapping panel for the dissection of complex traits in mice. *Genome Res* 20: 281–290, 2010. doi:10.1101/gr.099234.109.
- Bianchi ME. DAMPs, PAMPs and alarmins: all we need to know about danger. *J Leukoc Biol* 81: 1–5, 2007. doi:10.1189/jlb.0306164.
- Brusselle GG, Joos GF, Bracke KR. New insights into the immunology of chronic obstructive pulmonary disease. *Lancet* 378: 1015–1026, 2011. doi:10.1016/S0140-6736(11)60988-4.

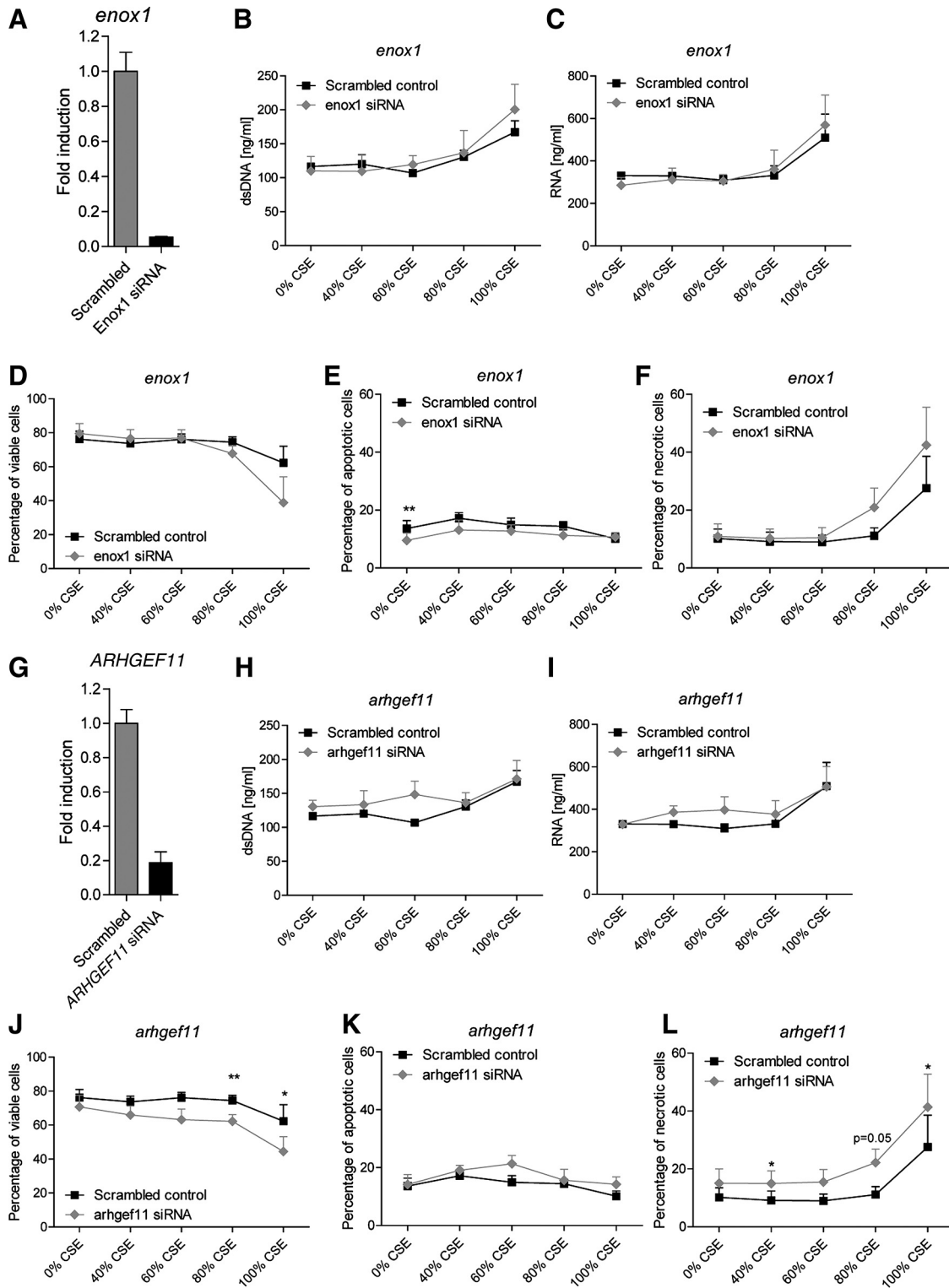


Fig. 11. The effect of downregulation of *ENOX1* and *ARHGEF11* on damage-associated molecular pattern (DAMP) release and cell death in human alveolar epithelial cells. The level of downregulation of *ENOX1* (A) and *ARHGEF11* (G) in A549 cells on treatment with specific small interfering (si) RNA analyzed, as by quantitative RT-PCR, is shown. Data are shown as fold induction of mRNA expression of A549 cells treated with scrambled siRNA assay ($2^{-\Delta\Delta C_T}$) compared with A549 cells treated with specific siRNA assays ($2^{-\Delta\Delta C_T}$). The levels of double-stranded (ds) DNA (B and H) and RNA (C and I) were measured in cell-free supernatant of A549 cells exposed to 0–100% CSE. Scrambled control represents cells treated with scrambled siRNA assay, and *ENOX1*/*ARHGEF11* siRNA is treated with specific siRNA assays. The levels of viable (D and J), apoptotic (E and K), and necrotic (F and L) cells were analyzed in A549 cells on exposure to 0–100% CSE using annexin/propidium iodide staining for flow cytometry. Values are means \pm SE of the mean. Significance was tested using a Mann-Whitney U-test. * $P < 0.05$. ** $P \leq 0.01$.

7. Castaldi PJ, Cho MH, Litonjua AA, Bakke P, Gulsvik A, Lomas DA, Anderson W, Beaty TH, Hokanson JE, Crapo JD, Laird N, Silverman EK; COPDGene and Eclipse Investigators. The association of genome-wide significant spirometric loci with chronic obstructive pulmonary disease susceptibility. *Am J Respir Cell Mol Biol* 45: 1147–1153, 2011. doi:10.1165/rcmb.2011-0055OC.
8. Cho MH, Castaldi PJ, Hersh CP, Hobbs BD, Barr RG, Tal-Singer R, Bakke P, Gulsvik A, San José Estépar R, Van Beek EJ, Coxson HO, Lynch DA, Washko GR, Laird NM, Crapo JD, Beaty TH, Silverman EK; NETT Genetics, ECLIPSE, and COPDGene Investigators. A genome-wide association study of emphysema and airway quantitative imaging phenotypes. *Am J Respir Crit Care Med* 192: 559–569, 2015. doi:10.1164/rccm.201501-0148OC.
9. Cho S, Dawson G. Palmitoyl protein thioesterase 1 protects against apoptosis mediated by Ras-Akt-caspase pathway in neuroblastoma cells. *J Neurochem* 74: 1478–1488, 2000. doi:10.1046/j.1471-4159.2000.0741478.x.
10. Cho S, Dawson PE, Dawson G. Antisense palmitoyl protein thioesterase 1 (PPT1) treatment inhibits PPT1 activity and increases cell death in LA-N-5 neuroblastoma cells. *J Neurosci Res* 62: 234–240, 2000. doi:10.1002/1097-4547(20001015)62:2<234::AID-JNR8>3.0.CO;2-8.
11. Cho S, Dawson PE, Dawson G. Role of palmitoyl-protein thioesterase in cell death: implications for infantile neuronal ceroid lipofuscinosis. *Eur J Paediatr Neurol* 5, Suppl A: 53–55, 2001. doi:10.1053/ejpn.2000.0409.
12. Cosio MG, Saetta M, Agusti A. Immunologic aspects of chronic obstructive pulmonary disease. *N Engl J Med* 360: 2445–2454, 2009. doi:10.1056/NEJMra0804752.
13. Dawson G, Dawson SA, Marinzi C, Dawson PE. Anti-tumor promoting effects of palmitoyl: protein thioesterase inhibitors against a human neurotumor cell line. *Cancer Lett* 187: 163–168, 2002. doi:10.1016/S0304-3835(02)00403-2.
14. Ferhani N, Letuve S, Kozhich A, Thibaudou O, Grandsaigne M, Maret M, Dombret M-C, Sims GP, Kolbeck R, Coyle AJ, Aubier M, Pretolani M. Expression of high-mobility group box 1 and of receptor for advanced glycation end products in chronic obstructive pulmonary disease. *Am J Respir Crit Care Med* 181: 917–927, 2010. doi:10.1164/rccm.200903-0340OC.
15. Follit JA, San Agustín JT, Xu F, Jonassen JA, Samtani R, Lo CW, Pazour GJ. The Golgin GMAP210/TRIP11 anchors IFT20 to the Golgi complex. *PLoS Genet* 4: e1000315, 2008. doi:10.1371/journal.pgen.1000315.
16. Franciosi L, Postma DS, van den Berge M, Govorukhina N, Horvathovich PL, Fusetti F, Poolman B, Lodewijk ME, Timens W, Bischoff R, ten Hacken NHT. Susceptibility to COPD: differential proteomic profiling after acute smoking. *PLoS One* 9: e102037, 2014. doi:10.1371/journal.pone.0102037.
17. Fuerst PG, Bruce F, Tian M, Wei W, Elstrott J, Feller MB, Erskine L, Singer JH, Burgess RW. DSCAM and DSCAML1 function in self-avoidance in multiple cell types in the developing mouse retina. *Neuron* 64: 484–497, 2009. doi:10.1016/j.neuron.2009.09.027.
18. Galic M, Tsai F-C, Collins SR, Matis M, Bandara S, Meyer T. Dynamic recruitment of the curvature-sensitive protein ArhGAP44 to nanoscale membrane deformations limits exploratory filopodia initiation in neurons. *eLife* 3: e03116, 2014. doi:10.7554/eLife.03116.
19. Geng L, Rachakonda G, Morré DJ, Morré DM, Crooks PA, Sonar VN, Roti JLR, Rogers BE, Greco S, Ye F, Salleng KJ, Sasi S, Freeman ML, Sekhar KR. Indolyl-quinuclidinols inhibit ENOX activity and endothelial cell morphogenesis while enhancing radiation-mediated control of tumor vasculature. *FASEB J* 23: 2986–2995, 2009. doi:10.1096/fj.09-130005.
20. Gupta P, Soyombo AA, Atashband A, Wisniewski KE, Shelton JM, Richardson JA, Hammer RE, Hofmann SL. Disruption of PPT1 or PPT2 causes neuronal ceroid lipofuscinosis in knockout mice. *Proc Natl Acad Sci USA* 98: 13566–13571, 2001. doi:10.1073/pnas.251485198.
21. Handa P, Tupper JC, Jordan KC, Harlan JM. FLIP (Flice-like inhibitory protein) suppresses cytoplasmic double-stranded-RNA-induced apoptosis and NF- κ B and IRF3-mediated signaling. *Cell Commun Signal* 9: 16, 2011. doi:10.1186/1478-811X-9-16.
22. He MX, He YW. CFLAR/c-FLIPL: a star in the autophagy, apoptosis and necroptosis alliance. *Autophagy* 9: 791–793, 2013. doi:10.4161/auto.23785.
23. Heijink IH, Pouwels SD, Leijendekker C, de Bruin HG, Zijlstra GJ, van der Vaart H, ten Hacken NH, van Oosterhout AJ, Nawijn MC, van der Toorn M. Cigarette smoke-induced damage-associated molecular pattern release from necrotic neutrophils triggers proinflammatory mediator release. *Am J Respir Cell Mol Biol* 52: 554–562, 2015. doi:10.1165/rcmb.2013-0505OC.
24. Hoonhorst SJ, Timens W, Koenderman L, Lo Tam Loi AT, Lammers JW, Boezen HM, van Oosterhout AJ, Postma DS, Ten Hacken NT. Increased activation of blood neutrophils after cigarette smoking in young individuals susceptible to COPD. *Respir Res* 15: 121, 2014. doi:10.1186/s12931-014-0121-2.
25. Hou C, Zhao H, Liu L, Li W, Zhou X, Lv Y, Shen X, Liang Z, Cai S, Zou F. High mobility group protein B1 (HMGB1) in Asthma: comparison of patients with chronic obstructive pulmonary disease and healthy controls. *Mol Med* 17: 807–815, 2011. doi:10.2119/molmed.2010.00173.
26. Itoh M, Tsukita S, Yamazaki Y, Sugimoto H. Rho GTP exchange factor ARHGGEF11 regulates the integrity of epithelial junctions by connecting ZO-1 and RhoA-myosin II signaling. *Proc Natl Acad Sci USA* 109: 9905–9910, 2012. doi:10.1073/pnas.1115063109.
27. Jiang YY, Xiao W, Zhu MX, Yang ZH, Pan XJ, Zhang Y, Sun C-C, Xing Y. The effect of human antibacterial peptide LL-37 in the pathogenesis of chronic obstructive pulmonary disease. *Respir Med* 106: 1680–10689, 2012. doi:10.1016/j.rmed.2012.08.018.
28. Kanazawa H, Tochino Y, Asai K, Ichimaru Y, Watanabe T, Hirata K. Validity of HMGB1 measurement in epithelial lining fluid in patients with COPD. *Eur J Clin Invest* 42: 419–426, 2012. doi:10.1111/j.1365-2362.2011.02598.x.
29. Kang HM, Zaitlen NA, Wade CM, Kirby A, Heckerman D, Daly MJ, Eskin E. Efficient control of population structure in model organism association mapping. *Genetics* 178: 1709–1723, 2008. doi:10.1534/genetics.107.080101.
30. Kirby A, Kang HM, Wade CM, Cotsapas C, Kostem E, Han B, Furlotte N, Kang EY, Rivas M, Bogue MA, Frazer KA, Johnson FM, Beilharz EJ, Cox DR, Eskin E, Daly MJ. Fine mapping in 94 inbred mouse strains using a high-density haplotype resource. *Genetics* 185: 1081–1095, 2010. doi:10.1534/genetics.110.115014.
31. Kono H, Rock KL. How dying cells alert the immune system to danger. *Nat Rev Immunol* 8: 279–289, 2008. doi:10.1038/nri2215.
32. Kurosaki M, Bolis M, Fratelli M, Barzago MM, Pattini L, Perretta G, Terao M, Garattini E. Structure and evolution of vertebrate aldehyde oxidases: from gene duplication to gene suppression. *Cell Mol Life Sci* 70: 1807–1830, 2013. doi:10.1007/s00018-012-1229-5.
33. Leikauf GD, Concel VJ, Bein K, Liu P, Berndt A, Martin TM, Ganguly K, Jang AS, Brant KA, Dopico RA Jr, Upadhyay S, Cario C, Di YPP, Vuga LJ, Kostem E, Eskin E, You M, Kaminski N, Prows DR, Knoell DL, Fabisiak JP. Functional genomic assessment of phosgene-induced acute lung injury in mice. *Am J Respir Cell Mol Biol* 49: 368–383, 2013. doi:10.1165/rcmb.2012-0337OC.
34. Leikauf GD, Concel VJ, Liu P, Bein K, Berndt A, Ganguly K, Jang AS, Brant KA, Dietsch M, Pope-Varsalona H, Dopico RA Jr, Di YP, Li Q, Vuga LJ, Medvedovic M, Kaminski N, You M, Prows DR. Haplotype association mapping of acute lung injury in mice implicates activin a receptor, type 1. *Am J Respir Crit Care Med* 183: 1499–1509, 2011. doi:10.1164/rccm.201006-0912OC.
35. Leikauf GD, Pope-Varsalona H, Concel VJ, Liu P, Bein K, Berndt A, Martin TM, Ganguly K, Jang AS, Brant KA, Dopico RA, Upadhyay S, Di YP, Li Q, Hu Z, Vuga LJ, Medvedovic M, Kaminski N, You M, Alexander DC, McDunn JE, Prows DR, Knoell DL, Fabisiak JP. Integrative Assessment of Chlorine-induced Acute Lung Injury in Mice. *Am J Respir Cell Mol Biol* 47: 234–244, 2012. doi:10.1165/rcmb.2012-0026OC.
36. Li H-H, Li Q, Liu P, Liu Y, Li J, Wasserloos K, Chao W, You M, Oury TD, Chhinder S, Hackam DJ, Billiar TR, Leikauf GD, Pitt BR, Zhang L-M. WNT1-inducible signaling pathway protein 1 contributes to ventilator-induced lung injury. *Am J Respir Cell Mol Biol* 47: 528–535, 2012. doi:10.1165/rcmb.2012-0127OC.
37. López-Campos JL, Tan W, Soriano JB. Global burden of COPD. *Respirology* 21: 14–23, 2016. doi:10.1111/resp.12660.
38. Magna M, Pisetsky DS. The alarmin properties of DNA and DNA-associated nuclear proteins. *Clin Ther* 38: 1029–1041, 2016. doi:10.1016/j.clinthera.2016.02.029.
39. Marcos V, Zhou-Suckow Z, Önder Yildirim A, Bohla A, Hector A, Vitkov L, Krautgartner WD, Stoiber W, Griese M, Eickelberg O, Mall MA, Hartl D. Free DNA in cystic fibrosis airway fluids correlates with airflow obstruction. *Mediators Inflamm* 2015: 408935, 2015. doi:10.1155/2015/408935.

40. Merkel D, Rist W, Seither P, Weith A, Lenter MC. Proteomic study of human bronchoalveolar lavage fluids from smokers with chronic obstructive pulmonary disease by combining surface-enhanced laser desorption/ionization-mass spectrometry profiling with mass spectrometric protein identification. *Proteomics* 5: 2972–2980, 2005. doi:10.1002/pmic.200401180.
41. Miano JM. Myocardin in biology and disease. *J Biomed Res* 29: 3–19, 2015. doi:10.7555/JBR.29.20140151.
42. Nakamura H. Genetics of COPD. *Allergol Int* 60: 253–258, 2011. doi:10.2332/allergolint.11-RAI-0326.
43. Nemmar A, Raza H, Subramanian D, John A, Elwasila M, Ali BH, Adeghate E. Evaluation of the pulmonary effects of short-term nose-only cigarette smoke exposure in mice. *Exp Biol Med (Maywood)* 237: 1449–1456, 2012. doi:10.1258/ebm.2012.012103.
44. Oppenheim JJ, Yang D. Alarmins: chemotactic activators of immune responses. *Curr Opin Immunol* 17: 359–365, 2005. doi:10.1016/j.coi.2005.06.002.
45. Pauwels RA, Rabe KF. Burden and clinical features of chronic obstructive pulmonary disease (COPD). *Lancet* 364: 613–620, 2004. doi:10.1016/S0140-6736(04)16855-4.
46. Pouwels SD, Heijink IH, Brouwer U, Gras R, den Boef LE, Boezen HM, Korstanje R, van Oosterhout AJ, Nawijn MC. Genetic variation associates with susceptibility for cigarette smoke-induced neutrophilia in mice. *Am J Physiol Lung Cell Mol Physiol* 308: L693–L709, 2015. doi:10.1152/ajplung.00118.2014.
47. Pouwels SD, Heijink IH, ten Hacken NH, Vandenabeele P, Krysko DV, Nawijn MC, van Oosterhout AJ. DAMPs activating innate and adaptive immune responses in COPD. *Mucosal Immunol* 7: 215–226, 2014. doi:10.1038/mi.2013.77.
48. Pouwels SD, Heijink IH, van Oosterhout AJ, Nawijn MC. A specific DAMP profile identifies susceptibility to smoke-induced airway inflammation. *Eur Respir J* 43: 1183–1186, 2014. doi:10.1183/09031936.00127813.
49. Pouwels SD, Hesse L, Faiz A, Lubbers J, Bodha PK, Ten Hacken NH, van Oosterhout AJ, Nawijn MC, Heijink IH. Susceptibility for cigarette smoke-induced DAMP release and DAMP-induced inflammation in COPD. *Am J Physiol Lung Cell Mol Physiol* 311: L881–L892, 2016. doi:10.1152/ajplung.00135.2016.
50. Pouwels SD, Zijlstra GJ, van der Toorn M, Hesse L, Gras R, Ten Hacken NH, Krysko DV, Vandenabeele P, de Vries M, van Oosterhout AJ, Heijink IH, Nawijn MC. Cigarette smoke-induced necroptosis and DAMP release trigger neutrophilic airway inflammation in mice. *Am J Physiol Lung Cell Mol Physiol* 310: L377–L386, 2016. doi:10.1152/ajplung.00174.2015.
51. Repapi E, Sayers I, Wain LV, Burton PR, Johnson T, Obeidat M, Zhao JH, Ramasamy A, Zhai G, Vitart V, Huffman JE, Igl W, Albrecht E, Deloukas P, Henderson J, Granell R, McArdle WL, Rudnicka AR, Barroso I, Loos RJ, Wareham NJ, Mustelin L, Rantanen T, Surakka I, Imboden M, Wichmann HE, Grkovic I, Jankovic S, Zgaga L, Hartikainen A-L, Peltonen L, Gyllenstein U, Johansson A, Zaboli G, Campbell H, Wild SH, Wilson JF, Gläser S, Homuth G, Völzke H, Mangino M, Soranzo N, Spector TD, Polasek O, Rudan I, Wright AF, Heliövaara M, Ripatti S, Pouta A, Naluai AT, Olin A-C, Torén K, Cooper MN, James AL, Palmer LJ, Hingorani AD, Wannamethee SG, Whincup PH, Smith GD, Ebrahim S, McKeever TM, Pavord ID, MacLeod AK, Morris AD, Porteous DJ, Cooper C, Dennison E, Shaheen S, Karrasch S, Schnabel E, Schulz H, Grallert H, Bouatia-Naji N, Delplanque J, Froguel P, Blakey JD, Britton JR, Morris RW, Holloway JW, Lawlor DA, Hui J, Nyberg F, Jarvelin MR, Jackson C, Kähönen M, Kaprio J, Probst-Hensch NM, Koch B, Hayward C, Evans DM, Elliott P, Strachan DP, Hall IP, Tobin MD; Wellcome Trust Case Control Consortium; NSHD Respiratory Study Team. Genome-wide association study identifies five loci associated with lung function. *Nat Genet* 42: 36–44, 2010. doi:10.1038/ng.501.
52. Richie CT, Peterson C, Lu T, Hittelman WN, Carpenter PB, Legerski RJ. hSnm1 colocalizes and physically associates with 53BP1 before and after DNA damage. *Mol Cell Biol* 22: 8635–8647, 2002. doi:10.1128/MCB.22.24.8635-8647.2002.
53. Safa AR. Roles of c-FLIP in apoptosis, necroptosis, and autophagy. *J Carcinog Mutagen Suppl* 6: 1–9, 2013. doi:10.4172/2157-2518.S6-003.
54. Lo Tam Loi AT, Hoonhorst SJM, Franciosi L, Bischoff R, Hoffmann RF, Heijink I, van Oosterhout AJ, Boezen HM, Timens W, Postma DS, Lammers J-W, Koenderman L, Ten Hacken NH. Acute and chronic inflammatory responses induced by smoking in individuals susceptible and non-susceptible to development of COPD: from specific disease phenotyping towards novel therapy. Protocol of a cross-sectional study. *BMJ Open* 3: e002178, 2013. doi:10.1136/bmjopen-2012-002178.
55. Tardy C, Sabourdy F, Garcia V, Jalanko A, Therville N, Levade T, Andrieu-Abadie N. Palmitoyl protein thioesterase 1 modulates tumor necrosis factor alpha-induced apoptosis. *Biochim Biophys Acta* 1793: 1250–1258, 2009. doi:10.1016/j.bbamcr.2009.03.007.
56. van der Vaart H, Postma DS, Timens W, Hylkema MN, Willemse BW, Boezen HM, Vonk JM, de Reus DM, Kauffman HF, ten Hacken NH. Acute effects of cigarette smoking on inflammation in healthy intermittent smokers. *Respir Res* 6: 22, 2005. doi:10.1186/1465-9921-6-22.
57. Venkateswaran A, Sekhar KR, Levic DS, Melville DB, Clark TA, Rybski WM, Walsh AJ, Skala MC, Crooks PA, Knapik EW, Freeman ML. The NADH oxidase ENOX1, a critical mediator of endothelial cell radiosensitization, is crucial for vascular development. *Cancer Res* 74: 38–43, 2014. doi:10.1158/0008-5472.CAN-13-1981.
58. Wang C, Zhou G-L, Vedantam S, Li P, Field J. Mitochondrial shuttling of CAP1 promotes actin- and cofilin-dependent apoptosis. *J Cell Sci* 121: 2913–2920, 2008. doi:10.1242/jcs.023911.
59. Xiao W, Hsu Y-P, Ishizaka A, Kirikae T, Moss RB. Sputum cathelicidin, urokinase plasminogen activation system components, and cytokines discriminate cystic fibrosis, COPD, and asthma inflammation. *Chest* 128: 2316–2326, 2005. doi:10.1378/chest.128.4.2316.
60. Zhang Q, Raouf M, Chen Y, Sumi Y, Sursal T, Junger W, Brohi K, Itagaki K, Hauser CJ. Circulating mitochondrial DAMPs cause inflammatory responses to injury. *Nature* 464: 104–107, 2010. doi:10.1038/nature08780.